

F
N
P

JOURNAL
OF
FOOD
PROCESS
ENGINEERING

D.R. HELDMAN
and
R.P. SINGH
COEDITORS

FOOD & NUTRITION
PRESS, INC.

VOLUME 13, NUMBER 2

QUARTERLY

JOURNAL OF FOOD PROCESS ENGINEERING

Coeditors: **D.R. HELDMAN**, National Food Processors Association, 1401 New York Ave., N.W., Washington, D.C.
R.P. SINGH, Agricultural Engineering Department, University of California, Davis, California

Editorial

Board: **A.L. BRODY**, Princeton, New Jersey (1991)
SOLKE, BRUIN, Vlaardingen, 1 Nederland (1991)
M. CHERYAN, Urbana, Illinois (1990)
J.P. CLARK, Chicago, Illinois (1991)
R.L. EARLE, Palmerston, North New Zealand (1991)
B. HALLSTROM, Lund, Sweden (1992)
M. KAREL, New Brunswick, New Jersey (1992)
J.L. KOKINI, New Brunswick, New Jersey (1990)
M. LEMAGUER, Edmonton, Alberta, Canada (1990)
R.G. MORGAN, Glenview, Illinois (1990)
M. PELEG, Amherst, Massachusetts (1990)
M.A. RAO, Geneva, New York (1992)
S.S.H. RIZVI, Ithaca, New York (1991)
E. ROTSTEIN, Minneapolis, Minnesota (1991)
I. SAGUY, Minneapolis, Minnesota (1990)
S.K. SASTRY, Columbus, Ohio (1992)
W.E.L. SPIESS, Karlsruhe, Germany (1990)
J.F. STEFFE, East Lansing, Michigan (1992)
K.R. SWARTZEL, Raleigh, North Carolina (1991)
A.A. TEIXEIRA, Gainesville, Florida (1992)
G.R. THORPE, Victoria, Australia (1992)

All articles for publication and inquiries regarding publication should be sent to **DR. D.R. HELDMAN**, COEDITOR, *Journal of Food Process Engineering*, National Food Processors Association, 1401 New York Ave., N.W., Washington, D.C. 20005 USA; or **DR. R.P. SINGH**, COEDITOR, *Journal of Food Process Engineering*, University of California, Davis, Department of Agricultural Engineering, Davis, CA 95616 USA.

All subscriptions and inquiries regarding subscriptions should be sent to Food & Nutrition Press, Inc., 6527 Main Street, P.O. Box 374, Trumbull, CT 06611 USA.

One volume of four issues will be published annually. The price for Volume 13 is \$98.00 which includes postage to U.S., Canada, and Mexico. Subscriptions to other countries are \$115.00 per year via surface mail, and \$124.00 per year via airmail.

Subscriptions for individuals for their own personal use are \$78.00 for Volume 13 which includes postage to U.S., Canada, and Mexico. Personal subscriptions to other countries are \$95.00 per year via surface mail, and \$104.00 per year via airmail. Subscriptions for individuals should be sent direct to the publisher and marked for personal use.

The *Journal of Food Process Engineering* (ISSN: 0145-8876) is published quarterly (March, June, September and December) by Food & Nutrition Press, Inc.—Office of Publication is 6527 Main Street, P.O. Box 374, Trumbull, Connecticut 06611 USA. (Current issue is November 1990.)

Second class postage paid at Bridgeport, CT 06602.

POSTMASTER: Send address changes to Food & Nutrition Press, Inc., 6527 Main Street, P.O. Box 374, Trumbull, CT 06611.

JOURNAL OF FOOD PROCESS ENGINEERING

JOURNAL OF FOOD PROCESS ENGINEERING

Coeditors:

D.R. HELDMAN, National Food Processors Association, 1401 New York Ave., N.W., Washington, D.C.
R.P. SINGH, Agricultural Engineering Department, University of California, Davis, California.

Editorial Board:

A.L. BRODY, Schotland Business Research, Inc., Princeton Corporate Center, 3 Independence Way, Princeton, New Jersey
SOLKE, BRUIN, Unilever Research Laboratorium, Vlaardingen, Oliver van Noortland 120 postbus 114, 3130 AC Claardingen 3133 AT Vlaardingen, 1 Nederland
M. CHERYAN, Department of Food Science, University of Illinois, Urbana, Illinois
J.P. CLARK, Epstein Process Engineering, Inc., Chicago, Illinois
R.L. EARLE, Department of Biotechnology, Massey University, Palmerston North, New Zealand
B. HALLSTROM, Food Engineering Chemical Center, S-221 Lund, Sweden
M. KAREL, Department of Food Science, Rutgers, The State University, Cook College, New Brunswick, New Jersey
J.L. KOKINI, Department of Food Science, Rutgers University, New Brunswick, New Jersey
M. LEMAGUER, Department of Food Science, University of Alberta, Edmonton, Canada
R.G. MORGAN, Kraft, Inc., Glenview, Illinois
M. PELEG, Department of Food Engineering, University of Massachusetts, Amherst, Massachusetts
M.A. RAO, Department of Food Science and Technology, Institute for Food Science, New York State Agricultural Experiment Station, Geneva, New York
S.S.H. RIZVI, Department of Food Science, Cornell University, Ithaca, New York
E. ROTSTEIN, The Pillsbury Co., Minneapolis, Minnesota
I. SAGUY, The Pillsbury Co., Minneapolis, Minnesota
S.K. SASTRY, Department of Agricultural Engineering, Ohio State University, Columbus, Ohio
W.E.L. SPIESS, Bundesforschungsanstalt fuer Ernaehrung, Karlsruhe, Germany
J.F. STEFFE, Department of Agricultural Engineering, Michigan State University, East Lansing, Michigan
K.R. SWARTZEL, Department of Food Science, North Carolina State University, Raleigh, North Carolina
A.A. TEIXEIRA, Agricultural Engineering Department, University of Florida, Gainesville, Florida
G.R. THORPE, CSIRO Australia, Highett, Victoria 3190, Australia

Journal of FOOD PROCESS ENGINEERING

**VOLUME 13
NUMBER 2**

**Coeditors: D.R. HELDMAN
R.P. SINGH**

**FOOD & NUTRITION PRESS, INC.
TRUMBULL, CONNECTICUT 06611 USA**

© Copyright 1990 by
Food & Nutrition Press, Inc.
Trumbull, Connecticut USA

All rights reserved. No part of this publication may be reproduced, stored in a retrieval system or transmitted in any form or by any means: electronic, electrostatic, magnetic tape, mechanical, photocopying, recording or otherwise, without permission in writing from the publisher.

ISSN 0145-8876

Printed in the United States of America

CONTENTS

Natural Convection Heat Transfer Between Non-Newtonian Fluids and an Irregular Shaped Particle A. ALHAMDAN and S.K. SASTRY	113
Oxygen Transmission Rate of an Edible Methylcellulose Palmitic Acid Film D.C. RICO-PENA and J.A. TORRES	125
An Approach to Study and Model the Hydrodynamic Cleaning Effect B.-O. BERGMAN and C. TRAGARDH	135
Mathematical Analysis of Critical Parameters in Aseptic Particulate Processing Systems J.W. LARKIN	155
Changes in Partition Coefficients of Alcohols as Affected by the Presence of Various Food Solids S. CHUNG and R. VILLOTA	169

ห้องสมุดคณะวิทยาศาสตร์บริการ

๓๑ ๓๑๓.๒๕๓๔

NATURAL CONVECTION HEAT TRANSFER BETWEEN NON-NEWTONIAN FLUIDS AND AN IRREGULAR SHAPED PARTICLE¹

A. ALHAMDAN and S.K. SASTRY²

*The Ohio State University
Department of Agricultural Engineering
590 Woody Hayes Drive
Columbus, Ohio 43210*

Accepted for Publication February 26, 1990

ABSTRACT

Natural convection heat transfer was investigated between aqueous solutions of sodium carboxymethylcellulose (modeled as power law fluids) and a mushroom shaped particle, under transient conditions, with various initial temperature differences. Convective heat transfer coefficients (h) were observed to decrease over time due to thermal equilibration. The average value of h was significantly higher for heating (75 to 310 $w/m^2 \cdot C$) than for cooling (22 to 153 $w/m^2 \cdot C$), and decreased with increasing viscosity (CMC concentration). For the lower viscosity ranges, h increased significantly with increasing initial temperature difference. Correlations were developed between Nusselt number and generalized Rayleigh and Fourier numbers.

INTRODUCTION

Many food process applications, including thermal sterilization and precook processes, involve heat transfer between non-Newtonian fluids and solid particles. The mechanisms usually are complex combinations of natural and forced convection, the predominance of a particular mechanism being dependent on system design and operational conditions. In many cases, it is necessary to quantify the contribution of the natural convection component to the overall heat transfer.

¹Salaries and research support provided by State and Federal Funds appropriated to the Ohio Agricultural Research and Development Center, The Ohio State University. Approved as Journal Article No. 60-90. References to commercial products and trade names is made with the understanding that no discrimination and no endorsement by The Ohio State University is implied.

²Author to whom correspondence is to be addressed.

Studies on natural and mixed convection about particles include those of Yuge (1960), Klyachko (1963), Kirk (1984), Moon (1984), and Johnson *et al.* (1987) for regular-shaped objects (mostly spheres) and air; and Amato and Tien (1972) for spheres and water. Studies on more applied retorting situations include those of Lenz and Lund (1978), Sastry (1984) and Fernandez *et al.* (1988). These studies deal primarily with Newtonian carrier fluids. Studies on heat transfer to non-Newtonian fluids have included those of Metzner and Friend (1959), Carreau *et al.* (1966) Mitsuishi and Miyari (1973), Jowitt and McCarthy (1974), and Anantheswaran and Rao (1985) for various forced and mixed convection situations in process equipment. The importance of natural convection heat transfer to Newtonian and non-Newtonian fluids in a Steritort was demonstrated by Rao *et al.* (1985). Other recent studies on natural or mixed convection are those of Chau and Snyder (1988), Chandarana *et al.* (1988, 1989), and Chang and Toledo (1989).

The natural convection component of heat transfer between particles and non-Newtonian fluids needs further characterization. In particular, convective heat transfer coefficients for many real processes need to be time-dependent functions, since natural convection driving forces change as equilibration occurs. Additional items requiring characterization are the differences in heat transfer rates between heating and cooling situations, and the effect of irregular shapes.

The motivation behind the present paper was primarily the *basic* interest in the question of natural convection heat transfer between non-Newtonian fluids and particles, the results of which would yield insight into the contribution of the natural convection component during processing. The objective was the measurement of natural convective heat transfer coefficients for still mushroom-shaped particles immersed in still power law fluids during heating and cooling processes.

MATERIALS AND METHODS

Principle

The particle used in this experiment was made of aluminum, and was in the shape of a mushroom, with cap diameter 0.0281 m, cap height 0.0159 m, and total height 0.0377 m. A copper-constantan thermocouple was imbedded in its interior (near the geometric center of cap). The use of a high conductivity material for the particle ensured that Biot numbers (based on preliminary experiments) were less than 0.1, so that the Newtonian heating and cooling law could be used for analysis of data. Thus, by monitoring the temperature of the object and that of the surrounding fluid over time, the heat transfer coefficient (h) could be determined from the relation:

$$\ln (T_{\text{obj}} - T_c) = \ln (T_i - T_c) - (hA/mC_p) t \quad (1)$$

From the experimental data, plots of $\ln(T_{\text{obj}} - T_c)$ versus time can be made. The slopes determined using least square methods yield:

$$h = -\text{slope} (mC_p/A)$$

After determination of h values, the Biot numbers were recalculated to verify the validity of the procedure.

Test Fluids

Aqueous solutions of sodium carboxymethylcellulose (CMC) were prepared at different concentrations to simulate non-Newtonian liquid foods. CMC powder was added to water to make three levels of concentration 0.5, 0.8, and 1.2%. Following each heat transfer experiment, rheological properties were determined at 20, 40 and 80 °C using a coaxial cylinder viscometer (Contraves RHEOMAT Model 115, Contraves AG, Zurich, Switzerland) equipped with a jacket for temperature control. Data were fitted to the Ostwald-de Waele power law model:

$$\tau = K\dot{\gamma}^n \quad (2)$$

Values of consistency coefficient (K) and flow behavior index (n) for each test condition are presented in Table 1.

TABLE 1.
RHEOLOGICAL PROPERTIES (FLOW BEHAVIOR INDEX, n AND CONSISTENCY COEFFICIENT K ; Pa sⁿ) OF CMC SOLUTIONS OF CONCENTRATION 0.5, 0.8, AND 1.2% AT TEMPERATURES 20, 40, and 80 °C

CMC Conc. %	Temperature (°C)					
	20		40		80	
	n	K	n	K	n	K
0.5	1.000	0.021	0.938	0.018	0.996	0.001
0.8	0.740	0.388	0.838	0.149	0.943	0.011
1.2	0.674	0.921	0.764	0.325	0.893	0.032

Experimental Procedure

The equipment consisted of two water baths, a data logger, a microcomputer, and the transducer particle. Electrical heaters were used to increase and control the temperatures of the two water baths at different, constant levels. Beakers

(800 mL) filled with test solution were suspended in each bath to act as the test chamber, and to protect against fluid movement and vibration due to the heater pump. Both baths were insulated to reduce heat loss. The particle surface was cleaned and polished before each run to prevent surface fouling.

The procedure for this experiment was to move the particle from one bath and immerse it in test liquid in the second water bath at a different temperature. For all studies, the particle was oriented with the stem end upward. The temperatures of the particle center and the two baths were recorded at 0.5 s interval during this process. The particle was transferred from bath to bath with care and as fast as possible to minimize heat loss from the particle to the air. This procedure of alternating movement between baths permitted collection of natural convection data for both heating and cooling.

The experiments were conducted such that each test fluid (0.5, 0.8 and 1.2% CMC solution) was used for heating and cooling process in the temperature ranges from 20 to 40 °C and 20 to 80 °C. Six replicates were done for each set of experimental variables resulting in seventy-two runs.

Fluid Velocities. To gain additional insight into the natural convection process, the velocity of the fluid around the particle due to temperature difference in the CMC medium was estimated by the following procedure. Tiny grains (ground polystyrene) were mixed with the CMC solution and a video camera was used to record the movement of these grains during a typical heat transfer test. A scale was mounted adjacent to the beaker to determine distances transversed by the grains, and the timer function of the camera was used to determine elapsed time. Velocities (within 0.5 to 1 cm of the particle surface) were determined during video replay by determining the distance traversed by the grains and the time elapsed. Velocities of twenty grains were studied under each condition of test. The data so obtained were not only useful for validating heat transfer findings, but also necessary in the determination of generalized Grashof and Rayleigh numbers as detailed in the data analysis section.

Data Analysis

Time-dependent heat transfer coefficients were determined by analyzing the temperature history plots in short segments (five data points each) and calculating heat transfer coefficients for each segment over time. Data for the first 5 s of processing were deleted because of the agitation caused by immersion of the particle in the solution. In addition, data involving temperature differences less than 0.5 °C between particle and fluid were deleted because these were within thermocouple error limits. These h values were used to determine Nusselt number values and the average time (for each segment) to determine Fourier number. Regressions were then performed to relate Nusselt (Nu), generalized Rayleigh (Ra_g) and Fourier (Fo) numbers.

In addition, average heat transfer coefficients were determined for each complete run by plotting graphs of $\log (T_{obj}-T_e)$ versus time and determining slopes of the entire plot.

Generalized dimensionless numbers were determined for data analysis. These included the generalized Prandtl (Pr_g), Grashof (Gr_g) and Rayleigh (Ra_g) numbers, defined as follows (Skelland 1967). Physical properties of test fluids were either experimentally determined (ρ , K , n) or assumed to be that of water under similar conditions (k_f , β , C_p).

$$Pr_g = C_p K \{ (3n+1)/n \}^n 2^{n-1} / \{ 4v^{1-n} d^{n-1} k_f \} \quad (3)$$

$$Gr_g = g\beta\rho^2 (T_{obj}-T_e) d^3 / \{ [K \{ (3n+1)/n \}^n 2^{n-1} / \{ 4v^{1-n} d^{n-1} \}] \}^2 \quad (4)$$

$$Ra_g = g\beta\rho (T_{obj}-T_e) d^3 / (\alpha [K \{ (3n+1)/n \}^n 2^{n-1} / \{ 4v^{1-n} d^{n-1} \}]) \quad (5)$$

$$= Gr_g Pr_g$$

RESULTS AND DISCUSSION

Average h values for different CMC concentrations and temperature ranges for heating and cooling are summarized in Table 2. The average values ranged between 22.1 and 310 $w/m^2 \text{ } ^\circ C$ depending on the variables: the concentration of CMC solution, temperature difference range, and heating or cooling. Statistically, with .01 level of significance, heat transfer coefficients increased with decreasing CMC concentrations within the range of conditions studied. For example, a decrease in the concentration of CMC solution from 1.2 to 0.5% resulted in an increase in h from 57 to 200 $w/m^2 \text{ } ^\circ C$ (about 400% increase) when heating at the same temperature difference from 20 to 40 $^\circ C$. In addition, h increased with temperature range only with the lower viscosity fluids. The influence was significant for heating with 0.5% CMC and cooling with 0.5 and 0.8% CMC solutions, but not so for the other cases, indicating that at high CMC concentration, the high viscosity tends to overshadow influences of temperature gradient. Another interesting observation was the lower h values found for cooling than that for heating at the same temperature difference and CMC concentration. These effects were noted in previous studies on natural convection between water and irregular particles (Chau and Snyder 1988; Alhamdan *et al.* 1988).

TABLE 2.
AVERAGE HEAT TRANSFER COEFFICIENTS (h , $w/m^2\cdot^{\circ}C$) FOR VARIABLE
TEMPERATURE DIFFERENCES AND CONCENTRATION FOR HEATING AND COOLING
OF STILL MUSHROOM-SHAPED PARTICLE IMMERSSED IN STILL CMC SOLUTION

Temperature Range ($^{\circ}C$)	h ($w/m^2\cdot^{\circ}C$)	
	Heating	Cooling
	0.5% CMC	
20-40	200 ^{a,n}	71 ^{b,y}
20-80	310 ^{a,m}	153 ^{b,x}
	0.8% CMC	
20-40	148 ^a	27.7 ^{b,s}
20-80	178 ^a	71.9 ^{b,r}
	1.2% CMC	
20-40	57 ^a	22.1 ^b
20-80	75 ^a	29.1 ^b

Comparisons between heating/cooling: mean values in the same row followed by different letters (a,b) are significantly different ($p < 0.01$)

Comparison between temperature ranges within the same CMC concentration: mean values in the same column within the same CMC concentration followed by different letters (m,n; x,y; r,s) are significantly different ($p < 0.01$). Unmarked values in the same column are not significantly different.

Comparisons between CMC concentrations: all comparisons across CMC concentrations (with other treatment variables being held constant) are significantly different from each other.

The data on fluid velocities under each test condition (Table 3) uphold the trends observed in the heat transfer studies. The velocities increase with increasing temperature difference and decreasing CMC concentration; and are greater for heating than cooling. The differences observed for heating and cooling are likely a result of: (1) the lower fluid viscosity under heating conditions, resulting in greater fluid velocities; and (2) differences in the flow patterns about the particle, dictated partially by the irregularity of the particle shape. The net flow near the particle was downward (particle colder than fluid) during particle heating and upward during cooling (fluid colder than particle) as expected. More precise characterization of flow fields is possible using such techniques as laser Doppler anemometry; however, this is outside the scope of the present studies.

TABLE 3.
AVERAGE VALUES AND STANDARD DEVIATIONS OF FLUID VELOCITIES (m/s)
AROUND THE PARTICLE DURING COOLING AND HEATING OF THE PARTICLE
WITH DIFFERENT CMC SOLUTIONS

Temperature Range (°C)	Average Velocity (m/s) \pm Standard Deviation	
	Heating	Cooling
0.5% CMC		
20-40	0.0017 \pm 0.0005	0.0012 \pm 0.00036
20-80	0.0090 \pm 0.0014	0.0051 \pm 0.0013
0.8% CMC		
20-40	0.0006 \pm 0.0001	0.0005 \pm 0.00021
20-80	0.0061 \pm 0.0009	0.0025 \pm 0.0012
1.2% CMC		
20-40	0.0005 \pm 0.0001	0.0003 \pm 0.00008
20-80	0.0043 \pm 0.0005	0.0028 \pm 0.00104

Comparison with literature values of h for natural convection indicate that these data encompass the values reported by Chang and Toledo (1989) (127 to 159 $\text{w/m}^2\text{°C}$) for 35% sugar solution, and Chandarnaa *et al.* (1988) (55.6 to 89.5 $\text{w/m}^2\text{°C}$) for starch solutions and 64.7 to 107.1 $\text{w/m}^2\text{°C}$ for water). The data of Chandarana *et al.* (1989) are at the lower end and below the range of this study. However, it is not possible or even desirable to make meaningful comparisons of these studies, because the conditions of experiment and test fluids are different in each case.

The rheological properties of fluids have a major impact on the values of heat transfer coefficient. In the present studies, the consistency coefficients decreased with temperature, as expected, and (except for the 0.5% solution, which was close to Newtonian) the flow behavior index increased with temperature. The reason for the effects is not clear, and it is not certain whether or not the same trends would persist under ultra-high temperature conditions. The studies of Dail (1989) have indicated a decrease of flow behavior index with increasing temperature; however, those studies involved starch solutions and the conditions of test differed from those of the present studies.

Values of the Biot number for each test condition are summarized in Table 4. These data support the validity of the method used.

TABLE 4.
A SUMMARY OF AVERAGE BIOT NUMBER (Bi) VALUES FOR A
MUSHROOM-SHAPE PARTICLE IMMERSIED IN STILL CMC SOLUTION

Temperature Range (°C)	Heating	Cooling
		0.5% CMC
20-40	0.05	0.02
20-80	0.08	0.04
		0.8% CMC
20-40	0.04	0.007
20-80	0.05	0.02
		1.2% CMC
20-40	0.01	0.006
20-80	0.02	0.008

A correlation of $\log Nu$ (utilizing time-dependent heat transfer coefficients) versus $\log Ra_g$ is plotted in Fig. 1. Increased Ra_g resulted in an increase of Nu for heating and cooling curves with Nu and Ra_g values being higher for the heating curve than for the cooling curve. The correlation can be expressed as follows:

For heating,

$$Nu = 1.88 \times 10^{-3} Ra_g^{.388}; \quad r^2 = .971 \quad (6)$$

For cooling,

$$Nu = 1.25 \times 10^{-1} Ra_g^{1.113}; \quad r^2 = .965 \quad (7)$$

The limits are $4.0 < Ra_g < 8.0$

Another correlation that relates h to elapsed time is the plot of $\log Nu$ versus Fo as shown in Fig. 2 in which Nu decreased with time. The results are as expected, since driving forces decrease with time due to equilibration. The resulting equations are:

For heating,

$$\log Nu = 3.11 - .077Fo; \quad r^2 = .977 \quad (8)$$

For cooling,

$$\log Nu = 1.59 - .037Fo; \quad r^2 = .977 \quad (9)$$

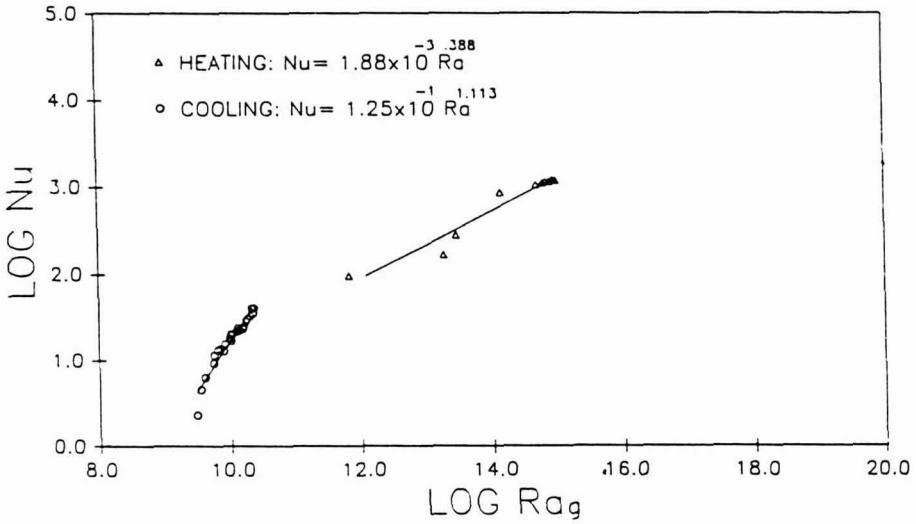


FIG. 1. PLOT OF NUSSLET NUMBER VERSUS RAYLEIGH NUMBER FOR HEATING AND COOLING OF MUSHROOM-SHAPE PARTICLE IMMERSED IN STILL CMC SOLUTION

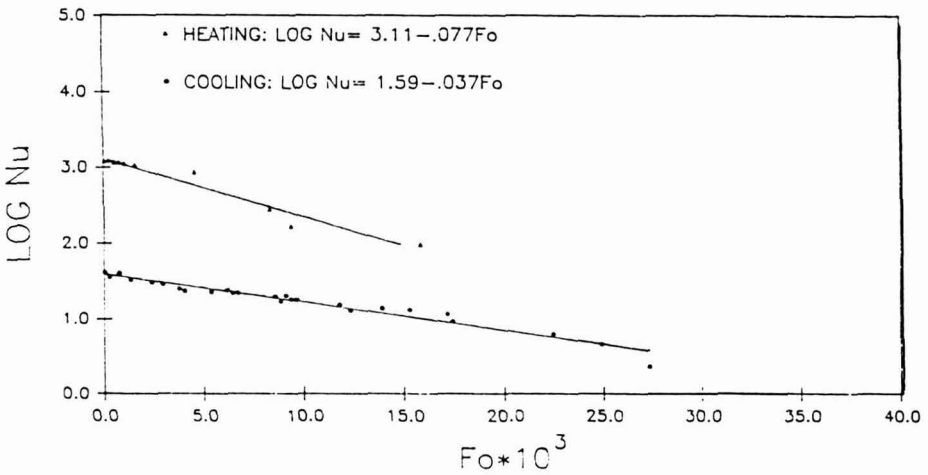


FIG. 2. PLOT OF NUSSLET NUMBER VERSUS FOURIER NUMBER FOR HEATING AND COOLING OF MUSHROOM-SHAPE PARTICLE IMMERSED IN STILL CMC SOLUTION

These results indicate the significant effects of the variation of CMC solution concentrations, temperature differences, and heating or cooling on heat transfer coefficient and process time.

CONCLUSIONS

Average heat transfer coefficients for natural convection between power law fluids (CMC solutions) and mushroom shaped particles ranged from 22.1 to 310 $\text{W/m}^2\text{ }^\circ\text{C}$ depending on test conditions. It was found that the average value of h increased with decreasing viscosity and increasing initial temperature difference. For the same range of experimental variables, h was higher for heating than for cooling, due at least partially to the lower fluid viscosity under the heating conditions. Fluid velocity about the particles also followed the same trends as the heat transfer results. The Nusselt number was found to decrease with time due to equilibration as expected.

LIST OF SYMBOLS

A	Surface area of the particle, m^2
C_p	Specific heat of the particle, $\text{J}/(\text{Kg } ^\circ\text{C})$
d	Equivalent particle (cap) diameter, m
g	Gravitational acceleration, m/s^2
h	Heat transfer coefficient, $\text{W}/\text{m}^2\text{ }^\circ\text{C}$
k_f	Thermal conductivity of fluid, $\text{W}/\text{m } ^\circ\text{C}$
K_s	Thermal conductivity of solid, $\text{W}/\text{m } ^\circ\text{C}$
K	Consistency coefficient of fluid, Pa s^n
m	Mass of the particle, Kg
n	Flow behavior index of fluid
r	Radius of cap, m
t	Time, s
T_e	Equilibration temperature, $^\circ\text{C}$
T_i	Initial temperature of the particle, $^\circ\text{C}$
T_{obj}	Temperature of particle center during process, $^\circ\text{C}$
v	medium velocity around the particle due to free convection, m/s

Greek Letters:

α	Thermal diffusivity of fluid = $\rho C_p / K_f$, m^2/s
β	Volumetric thermal expansion coefficient of fluid, $^\circ\text{C}^{-1}$
γ	Shear rate, s^{-1}
π	Mass density, Kg/m^3
τ	shear stress, Pa

Dimensionless Parameters:

- Bi Biot Number = hd/k_s
Fo Fourier Number = $\alpha t/d^2$
Gr_g Generalized Grashof Number (defined in Eq. 4)
Nu Nusselt Number = hd/k_f
Pr_g Generalized Prandtl Number (defined in Eq. 3)
Ra_g Generalized Rayleigh Number (defined in Eq. 5)

REFERENCES

- ALHAMDAN, A., SASTRY, S.K. and BLAISDELL, J.L. 1988. Experimental determination of free convective heat transfer from a mushroom-shape particle immersed in water. ASAE paper No. 88-6595, American Society of Agricultural Engineers, St. Joseph, MI.
- AMATO, W. and TIEN, C. 1972. Free convection heat transfer from isothermal spheres in water. *Int. J. Heat Mass Transfer* 15, 327-339.
- ANANTHESWARAN, R.C. and RAO, M.A. 1985. Heat transfer to model non-Newtonian liquid foods in cans during end-over-end agitation. *J. Food Engr.* 4, 21-35.
- CARREAU, P., CHAREST, G. and CORNIELLE, J.L. 1966. Heat transfer to agitated non-Newtonian fluids. *Can. J. Chem. Engr.* 44, 3-8.
- CHANDARANA, D.I., GAVIN, A., III and WHEATON, F.W. 1988. Particle/fluid interface heat transfer during aseptic processing of foods. ASAE Paper No. 88-6599. American Society of Agricultural Engineers, St. Joseph, MI.
- CHANDARANA, D.I., GAVIN, A., III and WHEATON, F.W. 1989. Simulation of parameters for modeling aseptic processing of foods containing particulates. *Food Technol.* 43(3), 137-143.
- CHANG, S.Y. and TOLEDO, R.T. 1989. Heat transfer and simulated sterilization of particulate solids in a continuously flowing system. *J. Food Sci.* 54(4), 1017-1023, 1030.
- CHAU, K.V. and SNYDER, G.V. 1988. Mathematical model for temperature distribution of thermally processed shrimp. *Transactions of the ASAE* 31(2), 608-612.
- DAIL, R.V. 1989. Rheological characterization of crosslinked waxy maize starch solutions under low acid aseptic processing conditions using tube viscometry techniques. M.S. Thesis, Michigan State University, East Lansing, MI.

- FERNANDEZ, C.L., RAO, M.A., RAJAVASIREDDY, S.P. and SASTRY, S.K. 1988. Particulate heat transfer to canned snap beans in a Steritort. *J. Food Proc. Engr.* 10, 183-198.
- JOHNSON, A., KIRK, G. and SHIH, T. 1987. Numerical and experimental analysis of mixed forced and natural convection about a sphere. *Trans ASAE* 31(1), 293-299, 304.
- JOWITT, R. and McCARTHY, O.J. 1974. The experimental determination of laminar flow heat transfer coefficients for Newtonian and non-Newtonian food liquids in tubular and plate heat exchangers. *Proc. IV Intl. Cong. Food Sci. & Technol.*, Madrid, Spain, Vol. 4, 350-360. Instituto de Agroquimicia y Tecnologia de Alimentos, Valencia, Spain.
- KIRK, G. 1984. Mixed convective heat transfer from spheres. M. S. Thesis, Agricultural Engineering Department, University of Maryland, College Park, MD 20742.
- KLYACHKO, L.S. 1963. Heat transfer between a gas and a spherical surface with the combined action of free and forced convection. *J. Heat Transfer* 85, 355-357.
- LENZ, M.K. and LUND, D.B. 1978. The lethality-Fourier number method. Heating rate variations and lethality confidence intervals for forced convection heated foods in containers. *J. Food Proc. Engr.* 2(3), 227-271.
- METZNER, A.B. and FRIEND, P.S. 1959. Heat transfer to turbulent non-Newtonian fluids. *Ind. Engr. Chem.* 51, 879-882.
- MITSUISHI, N. and MIYARI, Y. 1973. Heat transfer to non-Newtonian fluids in an agitated vessel. *J. Chem. Engr. Japan*, 6, 415-420.
- MOON, S. 1984. Analysis of combined natural and forced convection around cylinders and spheres. Ph.D. Dissertation, Agricultural Engineering Department, University of Maryland, College Park, MD 20742.
- RAO, M.A., COOLEY, H.J., ANANTHESWARAN, R.C. and ENNIS, R.W. 1985. Convective heat transfer to canned liquid foods in a Steritort. *J. Food Sci.* 50, 150-154.
- SASTRY, S. 1984. Convective heat transfer coefficients for canned mushrooms processed in still retorts. ASAE paper No. 84-6517.
- SKELLAND, A.H.P. 1967. *Non-Newtonian Flow and Heat Transfer*, John Wiley & Sons, New York.
- YUGE, T. 1960. Experiments on heat transfer from spheres including natural and forced convection. *J. Heat Transfer* 82, 214-220.

OXYGEN TRANSMISSION RATE OF AN EDIBLE METHYLCELLULOSE-PALMITIC ACID FILM¹

DELMY C. RICO-PÉÑA² and J. ANTONIO TORRES

*Food Engineering Group
Department of Food Science and Technology
Oregon State University
Corvallis, OR 97331*

Accepted for Publication April 4, 1990

ABSTRACT

Edible coatings with low potassium sorbate permeability could be used to increase the microbial stability of food surfaces. However, such coatings could induce anaerobic food conditions if their oxygen permeability were low. The oxygen permeability of an edible emulsion film (average thickness, 55 μm), composed of methylcellulose and palmitic acid (weight ratio of 3:1), was evaluated at 24°C, atmospheric pressure, and at different percentages of relative humidity (RH). RH values in the 0–57% range had no significant effect on oxygen transmission rate (OTR); calculated OTR values ranged from 660 to 740 mL O₂ (STP)/m² 24h atm. At 79% RH, the OTR doubled to 1,500 mL O₂ (STP)/m² 24h atm. This effect correlated well with the moisture isotherm for the film which showed a low moisture content in the 0–57% RH range and a rapid increase at higher RH values. OTR values, particularly at high relative humidity, indicate no risk of developing anaerobic conditions on the food surface.

INTRODUCTION

Oxygen permeability is a property of particular importance for the selection of food packaging materials. Many foods packaged in flexible films are sensitive to oxygen, and their shelf-life is determined largely by the oxygen permeability of the package (Davis and Burns 1969; Kester and Fennema 1986). Film composition, temperature and humidity affect the permeability to oxygen of films used for food packaging. Conditions of high relative humidity increase the

¹Oregon State University Experiment Station Publication No. 9121

²Author Rico-Pena is now with the Escuela de Ingenieria Quimica, Universidad de El Salvador, San Salvador, El Salvador

permeability of hydrophilic films, while hydrophobic materials are unaffected (Rigg 1979). Several methods are used for testing the permeability of flexible films to gases. Only permeability value ranges are given since unlike most analytical procedures no standardized methodologies are used (Karel *et al.* 1963; Davis and Huntington 1977; Rigg 1979).

Films of edible polysaccharide and fatty acids have been developed to extend product shelf-life. Kamper and Fennema (1984a,b; 1985) evaluated the permeability characteristics of these films to the transfer of moisture and focused on practical applications as moisture permeability barriers. Vojdani and Torres (1989; 1990) evaluated the permeability properties of polysaccharide-fatty acid films to the transfer of potassium sorbate, including the effect of temperature. These authors focused on the use of a coating/chemical preservative combination to improve the surface microbial stability of foods. Rico-Pena and Torres (1990) selected a methylcellulose-palmitic acid film formulation suggested by Vojdani and Torres (1990) and evaluated the effect of a_w and pH on preservative permeation rate.

The industrial application of a coating/chemical preservative combination requires data on the transfer of gases through the coating. For example, the availability of oxygen has an influence on the type of microbial spoilage of a food product. A low oxygen transmission rate could lead to the development of anaerobic conditions on the food surface. This would allow the growth of anaerobic pathogens.

In this paper we report on the effect of a_w on the oxygen transmission rate of a methylcellulose-palmitic acid film (weight ratio of 3:1). Food water activity (or environmental relative humidity) affect the hydration status of films and thus their permeability. The effect of a_w is interpreted on the basis of the moisture isotherm for the film.

MATERIALS AND METHODS

Reagents

Methyl cellulose (MC, Methocel A 15-LV, Premium) was donated by Dow Chemical Co. (Midland, MI). Palmitic acid (C16, 99%), polyethylene glycol 400 (PEG), potassium acetate, potassium carbonate, sodium bromide and ammonium chloride were purchased from Sigma Chemical Co. (St. Louis, MO). Potassium hydroxide, ammonium sulfate, potassium iodide, potassium nitrate, potassium chloride, sodium chloride, and potassium sulfate, all in analytical reagent quality, were purchased from VWR Scientific (Portland, OR). Ethanol (95%, reagent) was purchased from the OSU Chemical Store. Oxygen and nitrogen (pre-purified grade) gases were purchased locally (Industrial Welding Supply Inc., Corvallis, OR).

Film Preparation

Methyl cellulose-palmitic acid (MC-PA) films in a weight ratio of 3:1 were prepared by the emulsion technique described by Kamper and Fennema (1984a) and Vojdani and Torres (1989; 1990) using glass plates and a thin layer chromatography (TLC) applicator. The TLC applicator was set at 1.25 mm which resulted in films with a thickness of 52–56 μm . Films were dried at 90–95 °C for 15 min.

Film Thickness

The thickness of the films was measured using a top mounted Best Test Indicator (EDP No. 45987, Brown and Sharp Mfg. Co., N. Kingston, RI). Film thickness was measured after running the permeability test to avoid mechanical damage to the film when determining its thickness. Reported thickness values are the average of at least 20 measurements taken all over around the film area exposed to the permeation process.

Permeability Tests

The oxygen permeation rate of the MC-PA film was determined at 24 °C using a gas permeability cell (Fig. 1) similar to the one described by Davis and Huntington (1977). This cell operates on the concentration-increase principle developed by Landrock and Proctor (1952) and was custom built in Chile (Escuela Industrial, Valparaíso, Chile). The film was clamped between the two compartments. Two neoprene O-rings and vacuum grease were used as sealing aids to prevent gas leaking. The test compartment (lower compartment, 566 mL) was flushed with nitrogen for 2 h and, simultaneously, the upper compartment was flushed with the test gas, oxygen. After 2 h, gas flow from the supply cylinders was stopped. The inlet and outlet valves of the permeability cell were turned off in the mentioned order to ensure equal pressure (atmospheric pressure) in the two cell compartments as suggested by Davis and Huntington (1977).

At appropriate times, samples of gas (5 mL) were taken with a syringe from the test compartment. The increase in oxygen concentration was monitored using an oxygen head space analyzer (MOCON LC-700F, Minneapolis, MN). Five mL of nitrogen were added back to the lower cell compartment to replace the volume of gases removed during sampling and thus minimize changes in total pressure.

Relative humidity was controlled by passing each gas stream through a gas drying tower (0% RH). In the 20–80% RH range, the gases were passed first through a gas washing bottle containing distilled water to increase RH to 100%, followed by a second gas washing bottle containing a saturated salt solution corresponding to the required relative humidity condition, and finally through glass fiber to remove any saturated solution carry-over by the gas stream (Fig. 1). The

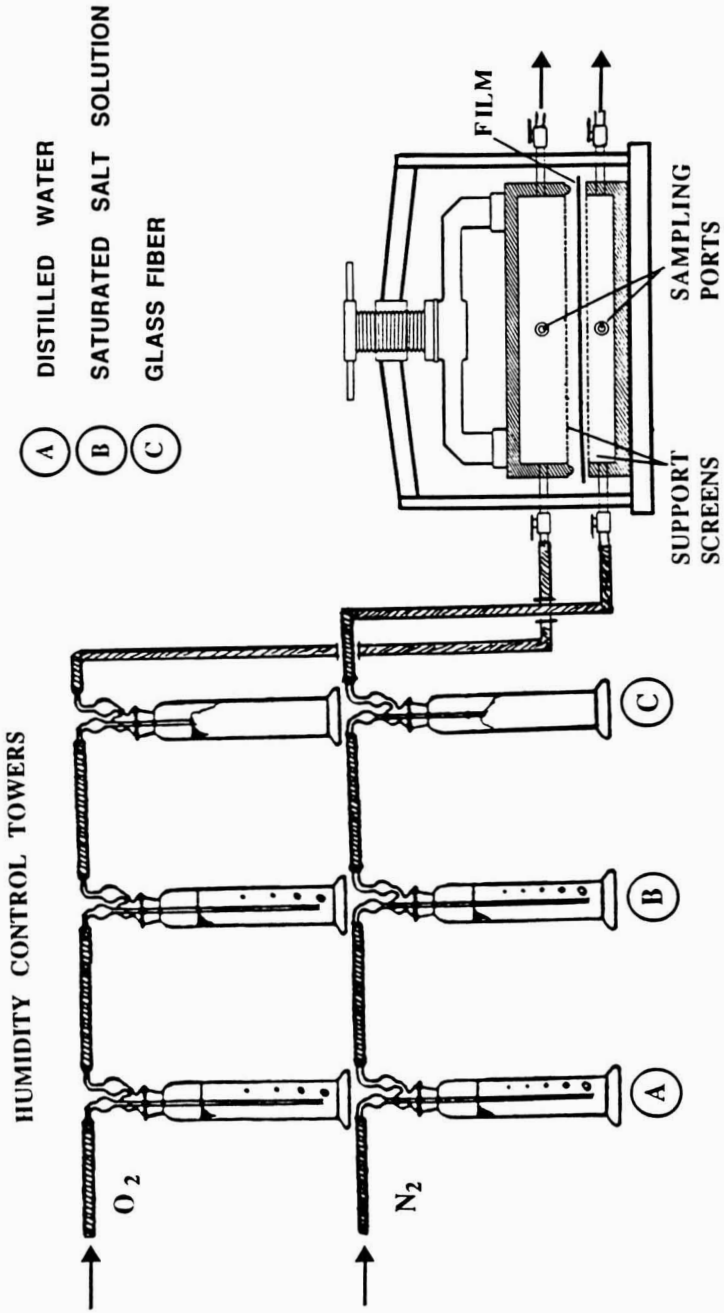


FIG. 1. SCHEMATIC REPRESENTATION OF THE OXYGEN PERMEABILITY CELL AND RELATED EQUIPMENT

saturated solutions used were potassium acetate (22% RH), potassium carbonate (43% RH), sodium bromide (57% RH) and ammonium chloride (79% RH) (Labuza 1984).

Determination of Oxygen Transmission Rate

Ideal gas behavior was assumed to correct oxygen concentration measurements because of the amount of oxygen lost during sampling and the 5 mL nitrogen added back to minimize pressure changes. Corrected O₂ data were plotted as a function of time. The slope of the linear portion of the curve was used to determine the amount of oxygen permeating per unit time at 24 °C and at the prevailing atmospheric pressure. The value was then recalculated as the volume of oxygen permeating per unit time at standard pressure and temperature conditions, and used to calculate the oxygen transmission rate by the following equation:

$$\text{OTR} = \frac{\text{Volume O}_2 \text{ (STP)}}{(\text{film area})(\text{time})(\text{pressure difference})}$$

OTR was expressed as mL O₂ (STP)/m² 24h atm for a film with a given thickness at a given temperature and % RH.

Determination of Film Moisture Isotherm

Triplicate samples of dehydrated MC-PA film were weighed and placed in tightly closed containers with a controlled RH environment and at 24 °C (Labuza 1984). Saturated salt solutions used to create the different %RH environments were potassium hydroxide (8% RH), potassium acetate (22% RH), potassium carbonate (43% RH), sodium bromide (57% RH), potassium iodide (69% RH), sodium chloride (75% RH), ammonium chloride (79% RH), ammonium sulfate (81% RH), potassium chloride (84% RH), potassium nitrate (94% RH) and potassium sulfate (97% RH) (Labuza 1984). After reaching moisture uptake equilibrium, individual samples were withdrawn from the containers and the increase in moisture content determined by weight difference.

Statistical Analysis

Statistical analysis of experimental data were done using Statgraphics (Version 3.0) on an IBM PS/2 model 30286.

RESULTS AND DISCUSSION

The amount of oxygen permeated as a function of time for a MC-PA film with an average thickness of 55 μm at 0, 22, 43, 57 and 79% RH (24 °C) is shown in Fig. 2. The calculated OTR values are shown in Table 1. RH values in the 0–57% range had no significant effect on oxygen transmission rate (OTR). Calculated OTR values ranged from 660 to 740 mL O₂ (STP)/m² 24h atm. At 79% RH, the OTR doubled to 1,500 mL O₂ (STP)/m² 24h atm. Statistical analysis showed this effect with a 95% confidence interval ($F_{\text{calculated}} = 812.8$, $F_{\text{tabulated}} = 5.19$; Devore and Peck 1986). Further analysis of multiple comparisons of means showed that the mean of OTR obtained at 79% RH was different from the means of OTR values obtained for 0, 22, 43 and 57% RH and that the means of OTR evaluated in the 0–57% RH range were not different from each other. This observation is consistent with earlier studies. Rico-Peña and Torres (1990) noted that the stability of MC-PA films is affected when exposed to environments with a_w 's higher than 0.80. The moisture sorption isotherm (Fig. 3) indicates that the moisture content of the film changes significantly at % RH larger than 50–60%. Therefore, OTR values as a function of RH agree well with the moisture uptake of the film as affected by RH conditions.

TABLE I.
OXYGEN TRANSMISSION RATE, MC-PA FILM, 24 °C

% RH ¹	Thickness μm	OTR mL O ₂ (STP)/m ² 24h atm
0	56	660
	52	700
22	55	710
	55	690
43	55	710
	55	720
57	55	740
	55	720
79	55	1,390
	55	1,400
	53	1,560

¹ Labuza 1984

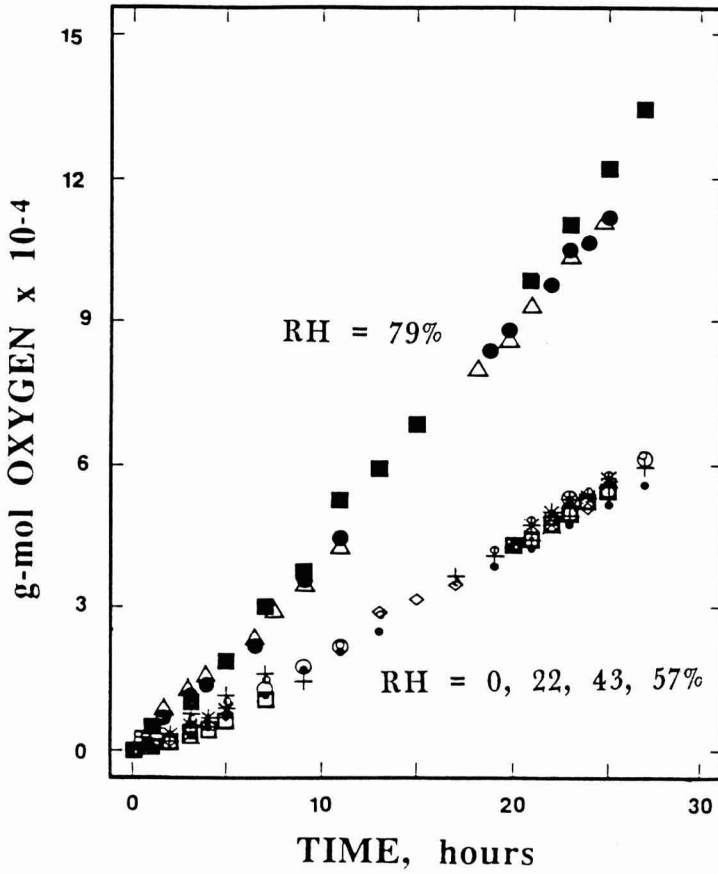


FIG. 2. EFFECT OF RELATIVE HUMIDITY ON THE OXYGEN PERMEABILITY OF AN EDIBLE METHYLCELLOSE-PALMITIC ACID FILM, WEIGHT RATIO OF 3:1, 24 °C

■, ●, △ = 80% RH; ○, □ = 60% RH; *, ◇, = 40% RH; □, □ = 20% RH; +, ● = 0% RH.

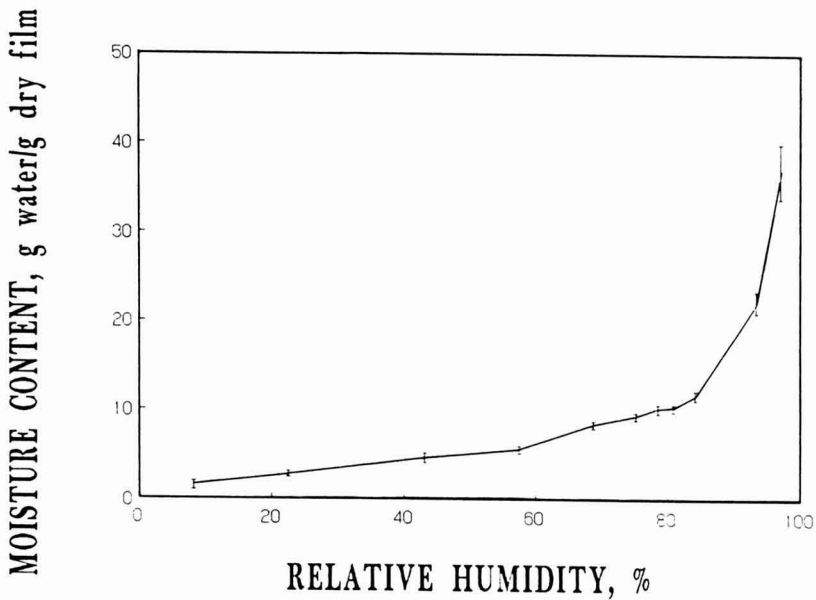


FIG. 3. MOISTURE SORPTION ISOTHERM OF A METHYLCELLULOSE-PALMITIC ACID FILM, WEIGHT RATIO OF 3:1, 24 °C

CONCLUSIONS

The MC-PA film is highly permeable to oxygen when compared to data reported in the literature for various other films (Anon. 1988; Rigg 1979; Davis 1964). OTR values, particularly at high relative humidity, indicate no risk of developing anaerobic conditions on the food surface.

More studies on the permeability to oxygen of the MC-PA film are needed. It is particularly recommended to evaluate the effect of temperature on OTR and analyze such data using the Arrhenius relationship. The successful application of this model would allow the determination of OTR values at any temperature.

ACKNOWLEDGMENTS

The authors are grateful for the equipment support of Oregon Freeze Dry, Inc. (Albany, OR). The help of Ingeniero J.A. Torres Z. on the design and construction of the permeability cell in Chile is also recognized. Author Rico-Peña gratefully acknowledges the support from the Fulbright-Latin American Scholarship Program of American Universities (LASPAU) and the Universidad de El Salvador.

REFERENCES

- ANONYMOUS. 1988. Films Division, Mobil Chemical Co., Pittsford, New York.
- DEVORE, J. and PECK, R. 1986. *Statistics: The Exploration and Analysis of Data*. pp. 681, West Publishing Co., Los Angeles.
- DAVIS, E.G. 1964. Oxygen permeability of nitrocellulose coated cellophane films. *Aust. J. Appl. Sci.* 15, 309.
- DAVIS, E.G. and BURNS, R.A. 1969. Oxygen permeability of flexible film packages for foods. *Food Technol.* 23(1), 92.
- DAVIS, E.G. and HUNTINGTON, J.N. 1977. New cell for measuring the permeability of film materials. *CSIRO Food Res. Q.* 37, 55.
- KAMPER, S.L. and FENNEMA, O.R. 1984a. Water vapor permeability of edible bilayer films. *J. Food Sci.* 49, 1478.
- KAMPER, S.L. and FENNEMA, O.R. 1984b. Water vapor permeability of an edible, fatty acid, bilayer film. *J. Food Sci.* 49, 1482.
- KAMPER, S.L. and FENNEMA, O.R. 1985. Use of an edible film to maintain water vapor gradients in foods. *J. Food Sci.* 50, 382.
- KAREL, M., ISSENBERG, P., RONSIVALLI, L. and JURIN, V. 1963. Application of gas chromatography to the measurement of gas permeability of packaging materials. *Food Technol.* 17(3), 91.
- KESTER, J.J. and FENNEMA, O.R. 1986. Edible films and coatings: A review. *Food Technol.* 40(12), 47.
- LABUZA, T.P. 1984. *Moisture Sorption: Practical Aspects of Isotherm Measurements and Use*. AACC. St. Paul, MN.
- LANDROCK, A.H. and PROCTOR, B.E. 1952. Simultaneous measurement of O₂ and CO₂ permeabilities of packaging materials. *TAPPI* 35(6), 241.
- RICO-PEÑA, D.C. and TORRES, J.A. 1990. Sorbic acid and potassium sorbate permeability of an edible methylcellulose-palmitic acid film: a_w and pH effects. *J. Food Sci.* Accepted for publication.
- RIGG, W.G. 1979. Measurements of the permeability of chilled meat packaging film under conditions of high humidity. *J. Food Technol. (U.K.)* 14, 149.
- VOJDANI, F. and TORRES, J.A. 1989. Potassium sorbate permeability of edible cellulose ether multi-layer films. *J. Food Proc. Pres.* 13, 417.
- VOJDANI, F. and TORRES, J.A. 1990. Potassium sorbate permeability of methyl cellulose and hydroxypropyl methylcellulose films: effect of fatty acids. *J. Food Sci.* 55, 841.

AN APPROACH TO STUDY AND MODEL THE HYDRODYNAMIC CLEANING EFFECT

BERT-OVE BERGMAN and CHRISTIAN TRAGARDH

*Division of Food Engineering,
University of Lund, Sweden*

Accepted for Publication May 2, 1990

ABSTRACT

A sensor has been developed for continuous measurements of the removal of deposit. The sensor, which was based on heat transfer measurements, was also able to measure the wall shear stress.

The device was used to study the mechanical effect during cleaning. It was found that the removal rate of deposits, at a surface, could be scaled by the mean wall shear stress. Measurements were performed under both laminar and turbulent flow conditions. The turbulent fluctuations did not influence the removal rate.

INTRODUCTION

The aim of cleaning is to remove all deposits and other unwanted substances which have soiled a system. In the food industry cleaning is an essential operation. At some plants such as dairies the equipment used for production consists of heat exchangers, valves, tanks, etc., connected through systems of pipes. Usually for the cleaning of such large equipment the cleaning solutions are pumped through the system, especially in those that cannot be taken apart. Thus cleaning-in-place (CIP), reduces a costly and time-consuming manual dismounting of the plant.

The cost of cleaning is influenced by several factors such as the price of cleaning chemicals, water consumption, energy consumption, nonproductive time, and labor costs. To minimize the costs the cleaning process must be optimized. One of the parameters to be optimized is the mass flow of cleaning solution. The flow of the cleaning solution transports chemicals and sometimes heat to the deposit, removes it from the surface, and functions as the transporting medium for removed deposit.

The cleaning rate is influenced by the type of deposit to be removed. Different foods and process parameters produce different types of deposit. As soon as cleaning chemicals start reacting with the deposit the properties of the deposit

are altered. However, in general, deposits can be regarded as particles, with sizes ranging from nanometers to millimeters, that are bound to the surface by different forces. Chemicals can reduce the magnitude of these forces. To remove a deposit a force of at least the same size as the force that binds the deposit to the surface must be applied.

Flow induces forces which act on the deposit on the surface. In food processing literature this phenomenon is called the mechanical effect or the hydrodynamic effect. The question as to how to characterize the mechanical effect can be formulated as follows: how are the removal forces created and what characterizes them?

In the literature various flow properties such as the Reynolds number, the average velocity and the mean wall shear stress have been used to characterize the mechanical effect. Most studies of cleaning rates have been performed using pipes or plate heat exchangers under turbulent flow conditions. Cleaver and Yates (1973) used the frequency and the size of coherent structures in the boundary layer to characterize the detachment of colloidal particles. According to Cleaver *et al.* (1973) the flow has to be turbulent in order to detach the deposit. Their hypothesis formed the basis for this work so as we considered it implausible that turbulence must be present. From this standpoint they suggest a model based on the existence of "bursts" in the turbulent boundary layer. The diameter of a burst was estimated to be $20 l^+$ and laterally distributed with a spacing of $135 l^+$. The axial distance between bursts was estimated to be $630 l^+$. The mean time between bursts was found to be $75 t^+ (\nu/u_\tau^2)$. They assumed that only a fraction of the surface beneath a burst was cleaned. That fraction was estimated to be 0.01. Thus, the fraction of the surface cleaned can be written as:

$$R(t) = 1 - \left[1 - \frac{0.01}{270} \right]^{(u_\tau^2 / 75 \cdot \nu) t} \quad (1)$$

where $R(t)$ is the probability percentage of the area of the surface cleaned. The initial cleaning rate can then be expressed as follows:

$$\frac{dR(0)}{dt} = - \frac{u_\tau^2}{75 \cdot \nu} \ln \left[1 - \frac{0.01}{270} \right] \quad (2)$$

For the case with constant fluid properties it can be written as

$$k_m = f(u_\tau^2) \quad (3)$$

Cleaver *et al.* also conclude that a particle will be removed only when

$$u_{\tau}^2 d_p^{\frac{4}{3}} > \text{Constant} \quad (4)$$

The above models and experiments are all for steady, well defined flow conditions.

Sediment transport in the sea or a river is a quite different case; here the flow is far from steady and the surface is generally rough. The normal approach to predicting sediment transport (Dyer and Soulsby 1988) is

$$k_m = f \left[(\rho_f u_{\tau}^2)^n \right], \quad (5)$$

where the exponent n normally lies in the range of 3/2 to 7/2. No transport takes place before a threshold value is exceeded. Equation 5 will then read

$$k_m = f \left[\left[\rho_f (u_{\tau}^2 - u_{\tau c}^2) \right]^n \right] \quad u_{\tau} > u_{\tau c} \quad (6)$$

and

$$k_m = 0 \quad \text{for} \quad u_{\tau} < u_{\tau c}$$

where $u_{\tau c}$ is the threshold friction velocity for motion.

METHODS AND MATERIALS

The Experimental Set-up

A stainless steel reservoir (Fig.1) with a volume of 0.7 m³ was connected to the pump (II) (Alfa Laval ALC 1/162, Lund, Sweden). The pump, which had a maximum capacity of 50 m³/h, was driven by a frequency converter so that the rotational speed could be varied between 0 – 2890 rpm. The magnetic flow meter (III) (Endress and Hauser Flowtec AG, Switzerland DI 670 – DN 40T,) had a measuring range from 0 m³/h to 20 m³/h, which corresponds to velocities from 0 m/s up to 1.0 m/s in the pipe (IV). At the entrance of the pipe a flow diffuser was placed, consisting of a 40 mm thick Plexiglas plate with 45 drilled holes 8 mm in diameter. The inner diameter of the pipe was 80 mm and the thickness of the wall was 5 mm. At both ends of the pipe conical constructions formed the transition between different diameters. The total length of the pipe, made of Plexiglas, was 6 m, which gives a length to diameter ratio of 75.

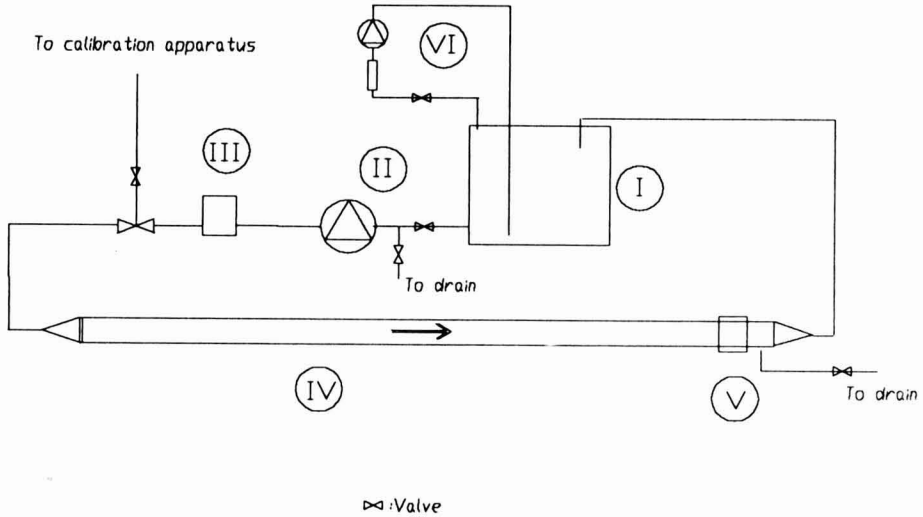


FIG. 1. SCHEMATIC DIAGRAM OF THE EXPERIMENTAL SET-UP
 I. Reservoir, II: Pump, III: Flow meter, IV: Pipe, V: Measuring station, VI: Filter system.

The measuring station (V) was placed 5.5 m, at $x/d = 69$ (length to diameter ratio) from the entrance. For measuring velocity at different radial distances from the wall a traversing equipment was used (see Fig. 2). The micrometer (Mitutoyo, Japan 297-101) had a resolution of $5 \mu\text{m}$ and was connected to the support of the probe (Dantec 55R15, Skovlunde, Denmark). At the bottom of the pipe two wall shear stress probes (TSI 1237W, St. Paul, MN, USA) were placed at $x/d = 69$. They were traversed normal to the wall which allowed the probes to be placed flush to the surface to within 0.02 mm. A stereo-microscope (Wild M1A 20 X 1, Switzerland) and a hair (from a brush) with a diameter of approximately 0.02 mm were used to place the probes flush with the surface.

On the probe support a thread was fastened and a nut was used to move the probe into position. It could be taken out through a specially designed valve without stopping the flow in the pipe.

A filter system (VI) was connected to the reservoir. A circulation pump then fed water from the bottom of the reservoir through the filter system (1 micron) and back into reservoir at the surface.

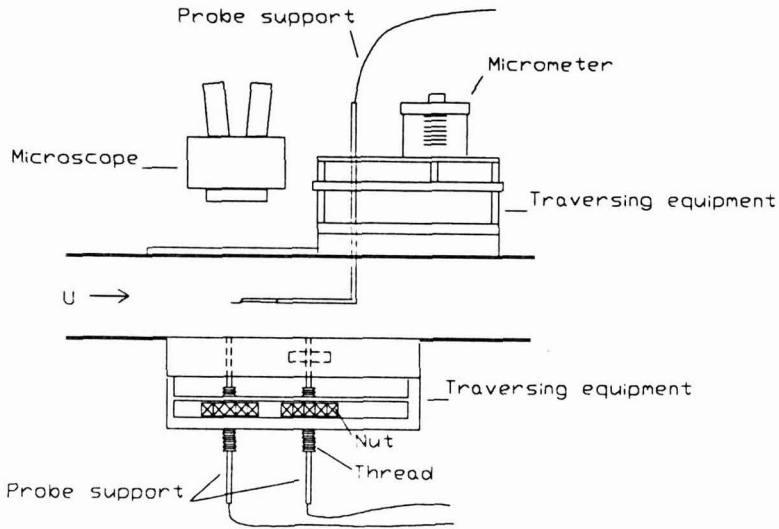


FIG. 2. THE MEASURING STATION. The drawing is not to scale.

Flow Modifiers

In order to obtain various conditions for the removal rate measurements the flow could be changed from the undisturbed case in two ways: (1) to lower the turbulence intensity and (2) to obtain laminar flow. Both of these modifications were made so that the same mean wall shear stress was obtained as for the undisturbed case.

To lower the turbulence level a streamlined piece of Plexiglas (see Fig. 3a) was placed on the probe support (the same as used for velocity measurements) and moved towards the wall. It was impossible to place it parallel to the wall, so that the distance between the wall and the flow modifier varied approximately between 0.7 and 1.5 mm.

To obtain laminar flow a cylinder (see Fig. 3 b) was placed just upstream of the measuring station. When the cylinder (Plexiglas) was placed in the pipe a channel was created between the wall and the flat side of the cylinder. The maximum height was 3 mm and the maximum width was 30 mm. The distance from the upstream end of the cylinder to the more downstream wall probe was approximately 400 mm.

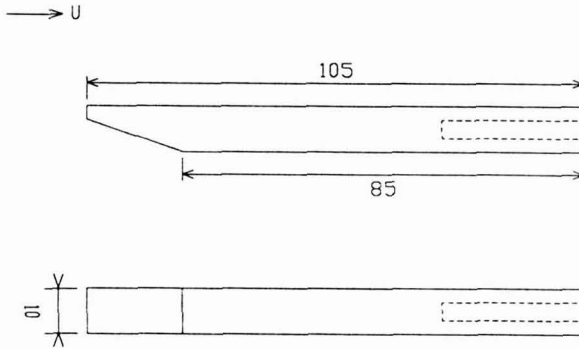


FIG. 3a. SCHEMATIC DIAGRAMS OF THE FLOW MODIFIER USED TO LOWER THE TURBULENCE INTENSITY.

It is made of Plexiglas. Size given in millimeters.

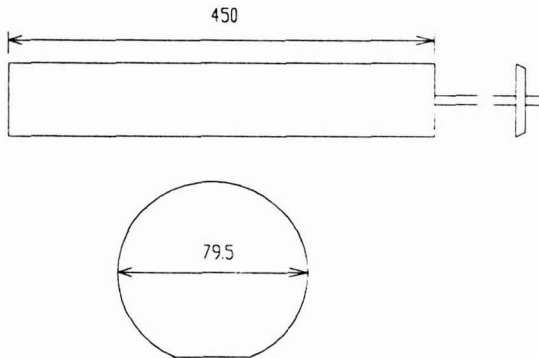


FIG. 3b. THE CYLINDER USED FOR CREATING LAMINAR FLOW IN THE PIPE

The drawing is not to scale. Size given in millimeters.

The Thermal Anemometer

The anemometer used in this study was Dantec 56 system (Skovlunde, Denmark). The system consists of two 56C17 CTA bridges, a 56N25 RMS unit (a true RMS voltmeter) and a mean value voltmeter 56N22. The settings on the bridge (filter and gain) were chosen according to the instructions in the Dantec manual, while the filter used on the bridge was 25 kHz.

Data Collecting System

The output signal from the anemometer was connected to a Lab Master board (Scientific Solutions, Inc), which has an A/D converter, timing facilities and multiplexer. The converter has a resolution of 12 bits and a programmable gain (1,2,4 and 8). The A/D unit has 16 channels. To set the time interval between the conversions the counter with a resolution of $1 \mu\text{s}$ was used. The board was controlled by a personal computer (IBM PC AT2). The maximum conversion rate was 10 kHz, if one channel was used.

Basic Equations

The deposit (in this case clay) was placed at the top of a sensor so that the heat transferred from the sensor to the fluid had to pass through the deposit. The clay then reduces the heat transferred from the sensor. The decrease in the rate of heat transfer was used to calculate the thickness of the clay.

With the constant temperature anemometer (CTA) the film (sensor) on the probe was kept at a constant temperature and the rate of heat transfer from the probe can be expressed as follows:

$$\frac{dq}{dt} = -R_s \cdot I^2 \quad (7)$$

and I is equal to

$$I = \frac{E}{(R_i + R_s + R_c)}$$

where E is the output voltage and R_s is the resistance of the sensor.

The rate of heat transfer from the surface of the deposit to the fluid is written

$$\frac{dq}{dt} = A \alpha (T_f - T_d) \quad (8)$$

where q is the energy, t is the time, A is the area of the sensor, α is the heat transfer coefficient, T_d denotes the temperature at the deposit/fluid interface and T_f denotes the temperature of the fluid (see Fig. 4). The rate of heat transfer through the deposit reads as follows:

$$\frac{dq}{dt} = \frac{A \cdot \lambda_d}{\ell} (T_d - T_s) \quad (9)$$

where ℓ is the thickness and λ_d is the thermal conductivity of the deposit. Combining substitution gives

$$\frac{\ell}{\lambda_d C_a} = \frac{1}{E^2} - \frac{1}{\alpha C_a} \quad (10)$$

where

$$C_a = A \cdot R_a \cdot (T_s - T_f)$$

and

$$\frac{1}{R_a} = \frac{R_s}{(R_i + R_s + R_c)^2}$$

The following variables have constant values under the experimental condition used: R_a , λ_d , T_s and T_f . The resistance R_a was kept constant by the anemometer and consequently the temperature of the sensor (T_s) was constant. The temperature of the fluid (T_f) was constant during the time it took to perform a series of experiments and since the temperature was constant the thermal conductivity (λ_d) was assumed to be constant.

To be able to use Eq. 10 to calculate the thickness of the deposit it was necessary to investigate the value of both α and A . The geometrical area of the sensor was 0.127 (mm²) and used here and α was measured under the conditions for the cleaning experiments.

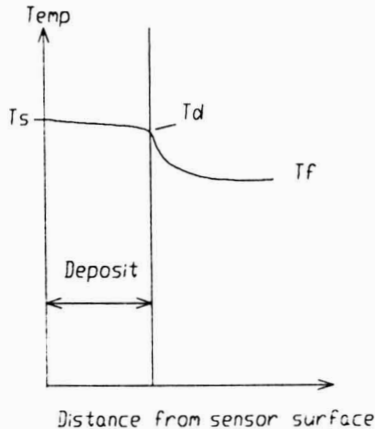


FIG. 4. THE TEMPERATURE PROFILE THROUGH THE CLAY LAYER AND IN ITS VICINITY

T_s denotes the temperature of the sensor, T_d the temperature at the clay/water interface and T_f the temperature of the fluid.

Experimental Procedure

The clay was made more homogenous by first making a suspension of it so that the larger particles settled out, pouring the suspension off and finally drying it at room temperature. With this method almost all particles $> 80 \mu\text{m}$ in diameter (as estimated under the microscope) were removed. Only two small samples of clay ($< 2.0 \text{ g}$) were used during the removal rate experiments.

To apply a thin layer of clay to the top of the probe, the probe was removed from the pipe, the tip was dipped into the clay and, by using a soft spatula, a thin layer was spread out over the top of the probe. The uniformity was judged by eye since if this was not done the removal of clay was affected by the nonuniform thickness of the clay.

The probe was then inserted by using the traversing mechanism so that the top of the probe was located a few millimeters below the inner wall of the pipe. The anemometer was turned on and the clay was heated to the temperature of the sensor. If the clay swells at all, it will do so during this period. After 1–2 min the probe was placed flush to the inner wall and the removal process started.

Figure 5 shows a typical removal process seen from above. At A the whole probe area is covered with clay. The removal process starts at the upstream edge, shown at B. As can be seen at C the clay is not removed evenly over the whole sensor, (the thickness of the clay varies over the sensor area). Therefore it was possible to measure only the average thickness of the clay over the sensor area.

Figure 6 shows the output voltage signal from the anemometer for a typical removal measurement. The first seconds are the end of the stabilization period when the clay was heated. During the first 7 to 15 s the probe was moved through the wall and placed flush with the surface to within 0.02 mm. The decrease of the signal during this period was not examined and was assumed to be of no importance. The removal process takes place between 15 and 70 s. At the beginning of this period the fluctuations of the voltage signal are low and increase as the thickness of the clay decreases. After 70 s all the clay had been removed and the voltage signal had a stable time average value. At the highest velocity used the removal process took about 20 s and the rate at which the voltage signal was sampled was 100 Hz.

The second term ($1/\alpha \cdot C_a$) of the right hand side of Eq. 10 was determined from the measurements with no deposit on the sensor, in order to be able to calculate the left hand side of Eq. 10. In Fig. 7 the same experiment as in Fig. 6 is presented in the form ($\ell/\lambda_d C_a$) versus time in seconds. The straight solid line represents a linear regression for the time between 15 to 70 s.

The value of the thermal conductivity λ_d was taken from Kersten (1949). The rate of heat transfer from the sensor was approximately 0.1 J/s.

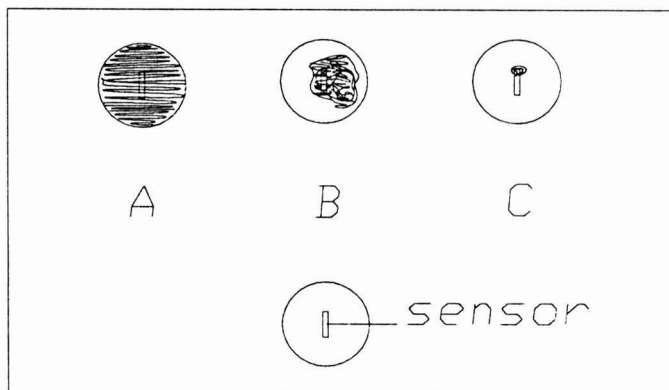


FIG. 5. A TYPICAL REMOVAL PROCESS SEEN FROM ABOVE. At A the whole probe is covered with clay and at C nearly all clay has been removed.

E

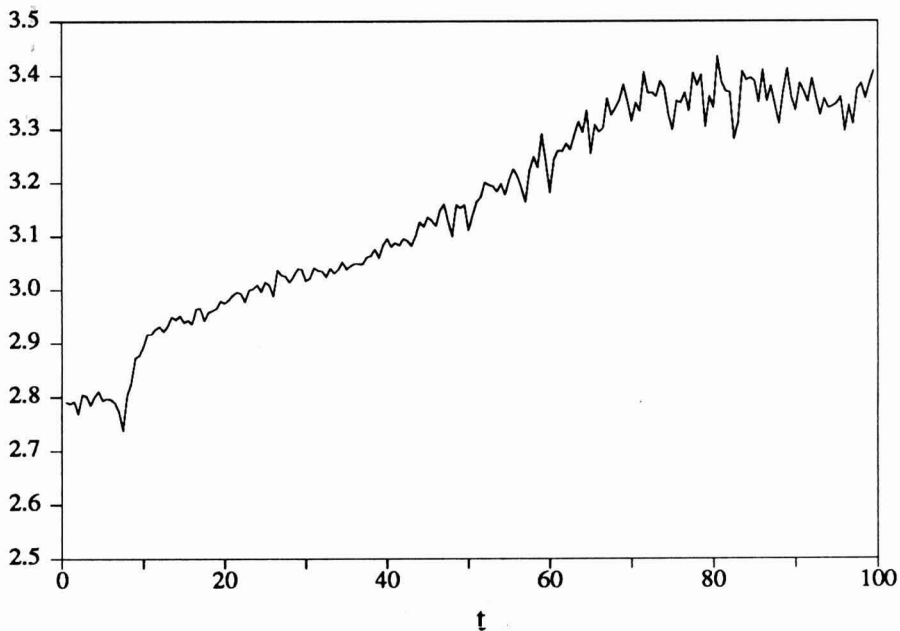


FIG. 6. THE OUTPUT VOLTAGE FROM THE ANEMOMETER DURING A TYPICAL REMOVAL PROCESS

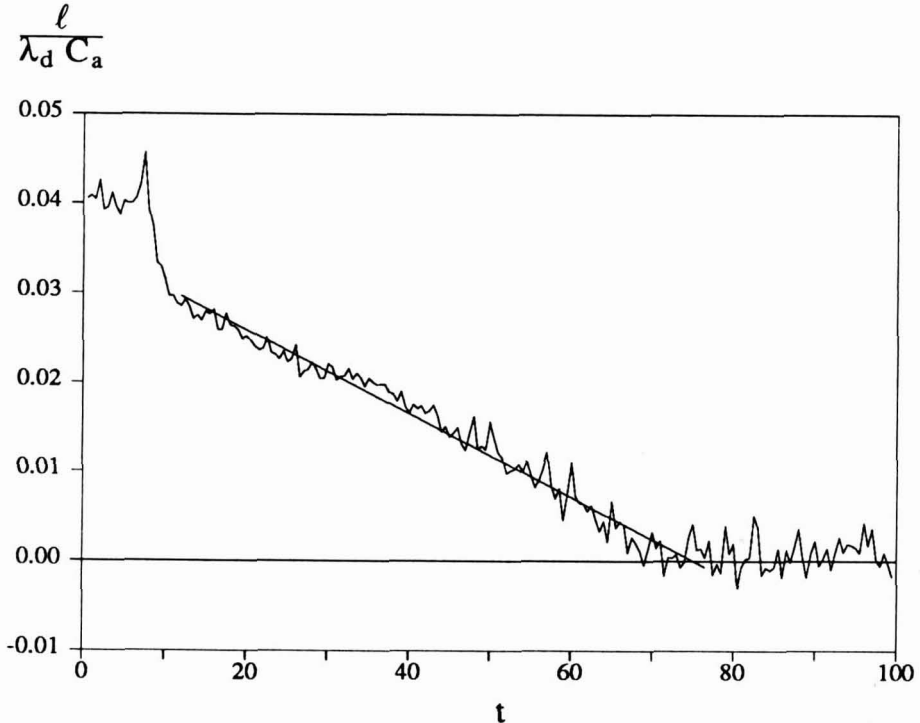


FIG. 7. THE THICKNESS OF THE LAYER (l) DIVIDED BY $\lambda_d \cdot C_a$ VERSUS TIME FOR A TYPICAL REMOVAL PROCESS

The solid line represents a linear regression for the time between 15 and 70 s. The removal rate is calculated from the slope.

RESULTS

Turbulent Flow Conditions

The removal rate was measured at six different mean wall shear stresses under fully developed turbulent pipe flow.

At a wall shear stress of 0.056 N/m^2 no removal occurs. The lowest wall shear stress at which the removal of clay was measured was 0.15 N/m^2 . In Fig. 7 three experiments are shown. The thickness of clay (l) multiplied by $1/\lambda_d C_a$ is plotted versus time. The starting point for the removal process is not the same for the different cases. The straight line is a linear regression of the data during the period of removal, and the slope of this line defines the removal rate. How well the regression fits the data is expressed as a correlation coefficient. The thickness of the clay was measured 100 times per second. The data were then integrated over periods of 4.0 s. As the integration time used affects the correlation coefficient, it was used only to compare experiments within a group. In Table 1 all experiments at a wall shear stress of 0.15 N/m^2 are presented. The mean removal rate was $0.037 \mu\text{m/s}$, with a standard deviation of $\pm 0.010 \mu\text{m/s}$.

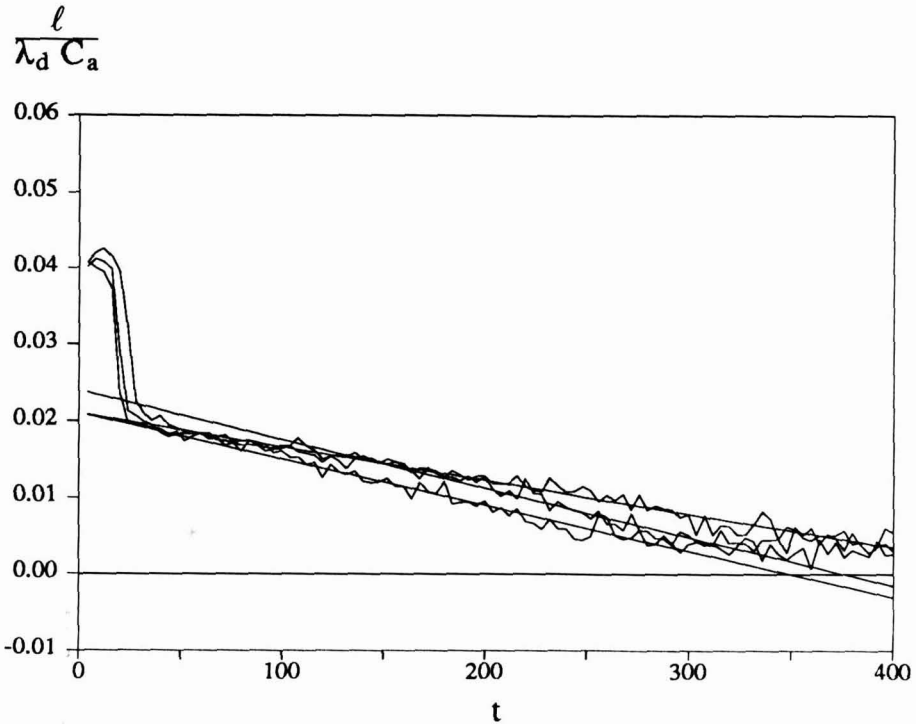


FIG. 8. THE RESULTS OF THREE REMOVAL EXPERIMENTS AT A MEAN WALL SHEAR STRESS OF 0.15 (N/m²)

TABLE 1.

THE REMOVAL RATE MEASURED AT A MEAN WALL SHEAR STRESS OF 0.15 N/m².

THE CONSTANT C_a HAS A VALUE OF $3.215 \cdot 10^{-4}$ AND $\lambda_d = 1.5$.

THE STANDARD DEVIATION FOR $d\ell/dt$ WAS ± 0.010 ($\mu\text{m/s}$).

THE CORRELATION COEFFICIENT IS CALCULATED FROM THE LINEAR REGRESSION.

Number	$-\frac{1}{\lambda_d C_a} \frac{d\ell}{dt}$ · 10 ⁴	$-\frac{d\ell}{dt}$ ($\mu\text{m/s}$)	Correlation coefficient
1	1.10	0.053	0.93
2	0.81	0.039	0.95
3	0.84	0.041	0.96
4	0.44	0.021	0.97
5	0.64	0.031	0.95
6	0.60	0.029	0.94
7	1.00	0.048	0.95
8	0.83	0.040	0.97
9	0.65	0.031	0.96
Mean value	0.77	0.037	0.95

The mean values and the standard deviation of the removal rate for the whole series of five experiments are presented in Table 2.

There is a tendency towards smaller relative standard deviations at higher mean wall shear stresses.

TABLE 2.
SUMMARY OF THE MEAN REMOVAL RATE MEASURED AT
DIFFERENT MEAN WALL SHEAR STRESSES IN A FULLY DEVELOPED TURBULENT
BOUNDARY LAYER. THE THIRD COLUMN SHOWS THE STANDARD DEVIATION
AND THE FOURTH THE RELATIVE STANDARD DEVIATION

τ_w	$-\frac{d\ell}{dt}$ ($\mu\text{m/s}$)	σ	$\sigma/(\frac{d\ell}{dt})$
0.15	0.037	0.01	0.27
0.30	0.085	0.017	0.20
0.72	0.231	0.024	0.10
1.28	0.496	0.078	0.16
2.00	0.920	0.110	0.12

Disturbed Turbulent and Laminar Flow Conditions

The turbulent boundary layer was disturbed with a flow modifier so that the turbulent intensity was decreased. This was done to see how the turbulent parameters influence the removal rate. The factor τ_w^3/\overline{T}_w was decreased from 0.32 to 0.09. Two experiments were performed; one under fully developed turbulent flow conditions and another under disturbed conditions. The mean wall shear stress was about the same in both experiments; for the fully developed case 0.8 N/m² and the disturbed case 0.74 N/m².

The water content of the clay was not the same as for the experiments presented in Table 2. The removal rate obtained above thus cannot be compared with those obtained in this section.

In Table 3 results from the three cases are summarized.

DISCUSSION AND CONCLUSIONS

Several authors have suggested that the removal of deposits from a surface is the rate limiting step in the cleaning process. In this case the influence of the flow on the cleaning rate should for particles be characterized by the mean wall shear stress, and by the average velocity if the deposit is considered as molecules.

TABLE 3.
SUMMARY OF THE MEAN REMOVAL RATE MEASURED AT DIFFERENT FLOW
CONDITIONS. THE THIRD COLUMN SHOWS THE STANDARD DEVIATION AND
THE FOURTH THE RELATIVE STANDARD DEVIATION

flow	T_w	$-\frac{d\ell}{dt}$ ($\mu\text{m/s}$)	σ	$\sigma/(\frac{d\ell}{dt})$
laminar	0.85	0.475	0.037	0.08
disturbed	0.73	0.408	0.046	0.11
turbulent	0.80	0.454	0.050	0.11

The models for cleaning kinetics, and the theory for the cleaning process have not been improved since the study of Jennings (1957). Almost all researchers agree that the cleaning process is complex, but nonetheless most studies have been performed under conditions where the whole process was involved. Consequently, in these studies great difficulties were encountered in separating the influence of the different phenomena involved (Jennings 1959; Hankinson *et al.* 1968 and Gallot-Lavallee *et al.* 1985).

In our opinion it is necessary to perform experiments on one such phenomenon at a time, before studying a combination. As an example: if two cleaning experiments are performed, having the same average velocity, but at different temperatures, many variables are changed, *e.g.*, viscosity, density, mean wall shear stress, reaction rate constants, diffusion coefficients and the properties of the deposit. How then can one determine which variables are the dependent ones?

The aim of measuring the removal rate of the deposit was to try to find a linear relationship between a flow parameter and the removal rate. The equation for such a relation reads

$$-\frac{d\ell}{dt} = C_1 \cdot X + C_2 \quad (11)$$

where X is a flow parameter or a function of a flow parameter, such as Re , U , T_w or the number of bursts, and ℓ stands for the thickness of the layer to be removed from the surface.

Experimental data used for these analyses, measured at fully develop turbulent pipe flow, are those presented in Table 2. Different choices of X were tested. No simple linear relationship was however obtained for example supporting the Cleaver and Yates theory. We thus started to analyze what mechanism is behind

the removal. Lifting force is one, shear force another. Hall (1988) measured the lifting force on particles in a turbulent boundary layer near the wall, and obtained data in good agreement with the following equation:

$$\frac{F}{v^2 \cdot \rho_f} = (20.9 \pm 1.57) \left[\frac{d_p \cdot u_\tau}{2 \cdot v} \right]^{2.31 \pm 0.02} \quad (12)$$

where F is the lifting force. Hall used particles with dimensionless diameters (d_p^+) between 3.6 to 140. By assuming that the lifting force and the removal rate are proportional, Eq. 12 can be written as

$$-\frac{d\ell}{dt} = \text{Const. } \bar{T}_w^{1.15} \quad (13)$$

for the case where d_p , v and ρ_f are constant, as in this investigation. No linear fit could be obtained when the removal rate is plotted *versus* $\bar{T}_w^{1.15}$. The intersection between the solid line and the x-axis is at a mean wall shear stress of 0.090. No removal occurs at a mean wall shear stress of 0.056. Therefore, Eq. 13 should be modified in the following way to fit the experimental data:

$$-\frac{d\ell}{dt} = C_1 \cdot \bar{T}_w^{1.15} + C_2 \quad \bar{T}_w > \bar{T}_{wc} = 0.090 \quad (14)$$

and

$$-\frac{d\ell}{dt} = 0 \quad \bar{T}_w < \bar{T}_{wc}$$

where

$$C_1 = 0.415, C_2 = -0.026$$

\bar{T}_{wc} is a removal threshold level.

This type of equation has also been found valid for sediment transport. The best fit of the experimental data was obtained by using this equation and determining the exponent by the least squares method. The value of the exponent obtained was 1.39, to be compared to 1.15 found by Hall (1988). The curve intersects the x-axis on its negative side. This is a nonphysical result, because experimentally no removal occurs at a mean wall shear stress of 0.056. The experiments show that

$$0.15 > \bar{T}_{wc} > 0.056$$

The exponent in Eq. 14 was calculated using the above condition for the threshold level, and the least squares method. The best fit was obtained for an exponent of 1.24. In Fig. 9 the removal rate is plotted *versus* $(\bar{T}_w)^{1.24}$, and the

solid line represents a linear regression. The experimental data are in good agreement with the equation

$$-\frac{d\ell}{dt} = C_1 \cdot (\bar{T}_w)^{1.24} + C_2 \quad \bar{T}_w > \bar{T}_{wc} = 0.057 \quad (14)$$

where

$$C_1 = 0.388, C_2 = -0.011.$$

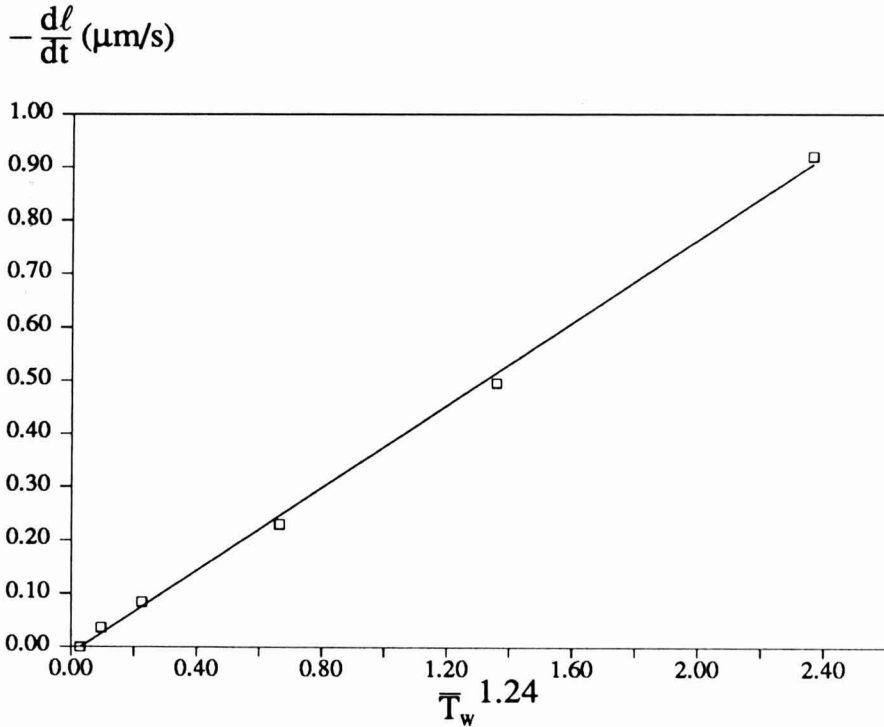


FIG. 9. THE REMOVAL RATE PLOTTED AS A FUNCTION OF $\bar{T}_w^{1.24}$
The solid line represents a linear regression

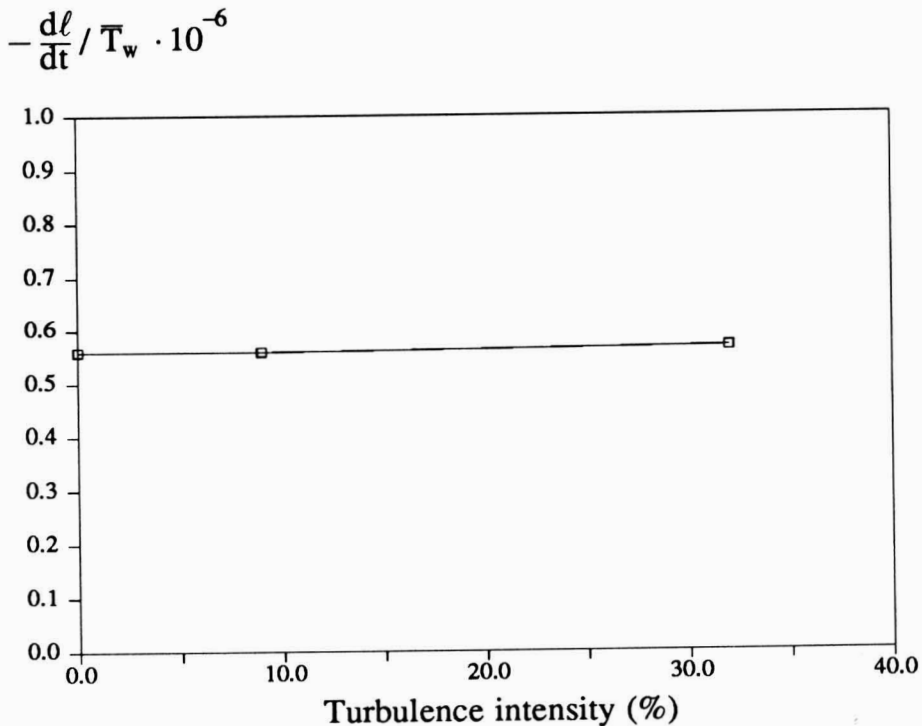


FIG. 10. THE REMOVAL RATE DIVIDED BY THE MEAN WALL SHEAR STRESS AS A FUNCTION OF THE TURBULENCE INTENSITY

The similarity between this equation and Hall's shows that this type of relation can be used to predict the removal rate of particles, and that the mean wall shear stress is a sufficient parameter. Hall used single spherical particles, and in the present experiments the size of the particles are not uniform, the largest particles being approximately $80 \mu\text{m}$ in diameter, and the smallest ones estimated to be $1 \mu\text{m}$ in diameter. The method used in the present study for measuring the removal rate cannot distinguish between those particles transported away from the surface and those transported along the surface. Hall measured the lifting force, which acts normal to the wall. Thus, the experimental conditions are different.

To investigate the influence of turbulent fluctuations on the removal rate, two experiments were performed:

(1) The turbulent intensity was decreased from 0.32 to 0.09 with the use of a flow modifier. It was not possible to calculate the values of the Reynolds numbers and the average velocities.

(2) The turbulence intensity was decreased and laminar flow was obtained.

These experiments were performed at approximately the same mean wall shear stress. These removal rates were compared with the removal rate obtained at fully developed turbulent pipe flow, and at the same mean wall shear stress. In Fig. 10 the removal rate divided by the mean wall shear stress is plotted *versus* the turbulence intensity. As can be seen from the figure, the turbulent fluctuations had no influence on the removal rate. The conclusion is that only mean values of flow parameters should be used to characterize the removal rate.

The practical importance, so far, of these results are related the possibility to analyse the response of changes in cleaning conditions to certain rate determining steps in the cleaning process. Equation 15 can be rearranged so that the removal rate is proportional to the mean flow velocity as (using the relationship $T_w = u_\tau^{2.0} \varrho$, $\Delta P = 4 T_w L/d$, $u_\tau = 0.2 U Re^{-1/8}$ and $Nu = Re^{0.8} Pr^{0.33}$)

$$-\frac{dl}{dt} \propto U^{2.17} \quad (16)$$

while that molecular mass transfer is

$$k_m \propto U^{0.8} \quad (17)$$

and for pressure drop

$$\Delta P \propto U^{1.75} \quad (18)$$

SYMBOLS

A	Area	m ²
C _i	Constant i = 1,2,3 etc.	
d _p	Diameter of particle	m
E	Voltage	
F	Lifting force	N
I	Current	
k _m	Mass transfer coefficient	kg/m ² s
l ⁺	Viscous length scale (ν/u_τ)	m
ℓ	Thickness of deposit	m
Nu	Nusselt number ($\alpha \cdot d/\lambda$)	
p	Pressure	N/m ²
Pr	Prandtl number ($c_p \cdot \eta/\lambda$)	
q	Energy	J

Ra	$(R_i + R_s + R_c)^2/R_s$	Ω
R_c	Resistance of cable	Ω
R_i	Resistance of anemometer bridge	Ω
R_s	Resistance of sensor	Ω
Re	Reynolds number ($U \cdot d/\nu$)	
T	Temperature	$^{\circ}\text{C}$
T_s	Temperature of sensor	$^{\circ}\text{C}$
T_d	Temperature of deposit/fluid interface	$^{\circ}\text{C}$
T_f	Temperature of fluid	$^{\circ}\text{C}$
\bar{T}_w	Mean wall shear stress	N/m^2
T_w	Wall shear stress	N/m^2
t^+	Viscous time scale (ν/u_{τ}^2)	
t	Time	s
U	Velocity in x direction	m/s
u_{τ}	Friction velocity	m/s
x	Cartesian coordinate	m
y	Cartesian coordinate	m
y^+	y/l^+	

Greek Symbols

α	Heat transfer coefficient	J/s m^2
τ_w^1	Mean fluctuating wall shear stress	N/m^2
λ_d	Thermal conductivity of deposit	$\text{J/s m } ^{\circ}\text{C}$
ρ	Density	kg/m^3
ρ_f	Density of fluid	kg/m^3
ρ_p	Density of particle	kg/m^3
ν	Kinematic viscosity	m^2/s
η	Viscosity	Ns/m^2

REFERENCES

- CLEAVER, J.W. and YATES, B. 1973. *J. of Colloid and Interface Sci.* 44, 464.
- CLEAVER, J.W. and YATES, B. 1976. *Chem. Eng. Sci.* 31, 147.
- DYER, K.R. and SOULSBY, R.L. 1988. *Ann. Rev. Fluid Mech.* 20, 295.
- GALLOT-LAVALLEE, T. and LALANDE, M. 1985. Proceedings 'Fouling and Cleaning in Food Processing', (D.B. Lund, E. Plett and C. Sandu, eds.) Madison, WI.
- HALL, D. 1988. *J. Fluid Mech.* 187, 451.

- HANKINSON, D.J. and CARVER, C.E. 1968. *J. Dairy Sci.* 51, 1761.
- JENNINGS, W.G. 1957. *J. Dairy Sci.* 40, 1471.
- JENNINGS, W.G. 1959. *J. Dairy Sci.* 42, 1763.
- KERSTEN, M.S. 1949. Thermal properties of soil. Inst. of Tech. Eng. Exp. Station, Bulletin No. 28, Minneapolis.
- PAULSSON, B.-O. 1989. Ph.D. thesis, Lund University Institute of Technology.

MATHEMATICAL ANALYSIS OF CRITICAL PARAMETERS IN ASEPTIC PARTICULATE PROCESSING SYSTEMS

JOHN W. LARKIN
Agricultural Engineer

*Food and Drug Administration
Food Engineering Branch
6502 S. Archer Rd.
Summit-Argo, IL 60501*

Accepted for Publication June 4, 1990

ABSTRACT

A sensitivity analysis of a one-dimensional heat transfer model for a heat-hold-cool aseptic system of food products containing particulates was completed for eighteen different design, product, and process control parameters. All of the parameters, except the direct effect of the fluid specific heat, were determined to be statistically significant in influencing the accumulated lethality of the processes. The most influential parameters were surface heat transfer coefficient in the hold tube at the fluid-particle interface, exit temperature of the fluid from the heater, initial temperature, holding tube size, and holding tube-U value. The process/product-related parameters that are significant in the establishment of a process are: particle diameter, surface heat transfer coefficient in the hold tube at the fluid-particle interface, thermal properties of the fluid and particulates, maximum heater velocity ratio, maximum hold tube velocity ratio, surface heat transfer coefficient in the heater at the fluid-particle interface, product flow rate, and particle to fluid ratio.

INTRODUCTION

Heat transfer into food products that are processed aseptically is dependent on a number of design, processing, and product-specific variables. Numerous computerized simulation models have been postulated for the heating of low-acid foods containing particulates in aseptic processing systems (de Ruyter and Brunet 1973; Manson and Cullen 1974; Sastry 1986; Castaigne and Lacroix 1987; Chandarana *et al.* 1989; Larkin 1989; and Lee *et al.* 1990). Sastry (1988) and Chandarana and Gavin (1989a) reviewed numerous simulation methods and their assumptions and limitations. The models developed by Sastry (1986) and Chandarana *et al.* (1989) account for more design, process, and product-dependent parameters than any of the other indicated models. The main benefit

of a simulation model is that it allows a user to easily and quickly investigate the amount of accumulated lethality for a given system and the influence of a change in processing conditions without the expense of an actual process run.

Using his own model, Sastry (1986) investigated the effect of (1) particle size, (2) residence time of the fastest particle within the scraped-surface heat exchanger (SSHE), (3) heat transfer coefficient at the fluid-particle interface (h), and (4) residence time of the fastest particle within the holding tube on the required minimum holding tube length in order to reach an F_0 of 8.0. Sastry's (1986) analysis was completed using a fixed heater, hold tube diameter, and target accumulated lethality (F_0). He observed that all of the parameters investigated influenced the necessary hold tube length. However, it was not until the surface heat transfer coefficient for the fluid-particle interface was half that for a typical brine fluid that its influence was significant. The largest effect of the four parameters investigated and for the ranges used was that of the residence time of the fastest particle in the hold tube.

Chandarana *et al.* (1989) and Chandarana and Gavin (1989b), using a model based on that developed by Sastry (1986), investigated the effect of (1) processing temperature, (2) particle size, (3) particle concentration, (4) surface heat transfer coefficient at the fluid-particle interface, (5) residence time of the fastest particle for both the heater and hold tube, and (6) particle thermal diffusivity. They performed their analysis for spherical, cylindrical, and cube-shaped particles, with most of the analysis completed on the cube-shaped particle. The system was designed for a fixed heater, hold tube diameter, hold tube length of specified F_0 , and fixed fluid exit temperature or heater steam temperature. All of the parameters investigated influenced the holding tube length of the system. When the thermal diffusivity of the particle was changed from $1.0 \times 10^{-7} \text{ m}^2/\text{s}$ to $1.5 \times 10^{-7} \text{ m}^2/\text{s}$, the holding tube length changed from 58 to 45 m. The residence time of the fastest particle in the hold tube was one of the most significant parameters. A change in percent of loading of particles (10–50%) resulted in the least influence of all the parameters studied.

Lee *et al.* (1990), using a simplified Sastry model (the liquid temperature profile was predefined and independent of particle loading), analyzed a typical aseptic system for changes in (1) the effective heater overall surface heat transfer coefficient, (2) the hold tube overall heat transfer coefficient, (3) fluid-particle surface heat transfer coefficient, (4) fastest particle residence time for both the heater and hold tube, and (5) particle thermal diffusivity. Because of the type of model used, Lee *et al.* (1990) found that if the exit temperature of the heater was controlled, a change in the overall surface heat transfer coefficient of the heater (SSHE-U) did not appreciably change the process time. This means that for a controlled and fixed exit temperature, any changes in the heating rate of the fluid (i.e., steam temperature, thermal properties, flow rate, and fouling) may not appreciably influence the process time. They also observed that the surface heat

transfer coefficient for the fluid-particle interface did not start to significantly influence the process time until it dropped below 500 W/m²°C. They found that as the velocity ratio (VR) of the fastest particle (particle velocity/average bulk velocity) for both the heater and hold tube reached 2.0 and above, the process time did not change appreciably. This does not mean that the length of the holding tube does not change as the velocity ratio changes; it means that once its velocity ratio reaches 2.0 for a given F₀, the total time that the fastest particle is in the system is about the same.

Each of these investigations allowed for some comparisons between the different parameters. However, the relative magnitude between each of the parameters could not be related. The objective of this research project was to determine the relative significance of known quantitative changes in each of 18 different design, process, and product specific parameters on the accumulated lethality at the center of the fastest moving particle of a given system.

MATERIALS AND METHODS

The model used for this study is similar to that presented by Sastry (1986) except that spherical instead of mushroomed-shaped particles were used and the exit temperature of the fluid from the heater was held constant by letting the steam temperature of the heater vary for the changing processing conditions (Eq. 1). For Eq. 1: T_i = uniform initial temperature of particle, T_∞ = fluid temperature at time = t, T_s = surface temperature of sphere, h_p = surface heat transfer coefficient at fluid-particle interface, k = thermal conductivity of particle, ρ = density of particle, C_p = specific heat of particle, R = radius of particle, and r = radial position within particle. Energy and mass balances were completed for both the heater and the hold tube sections to complete the development of the model using the following assumptions: (1) particles are of equal size (2) average particle flow rate is equal to the average mass flow rate of the fluid, (3) constant particle concentration throughout, (4) uniform cross sectional fluid temperature, (5) constant thermal and physical properties, (6) insulated condition at the SSHE shaft wall.

$$k \left[\frac{2}{r} \frac{\partial T}{\partial r} + \frac{\partial^2 T}{\partial r^2} \right] = \rho C_p \frac{\partial T}{\partial t}; \text{ when } 0 \leq r < R, t > 0 \quad (1)$$

$$k \frac{\partial T}{\partial r} = h_p [T_s - T_\infty(t)]; \text{ when } r = R, t > 0$$

$$T = T_i; \text{ when } 0 \leq r \leq R, t = 0$$

The main difference between Sastry's program and the one used here is that because of the unidirectional heating condition of a sphere, a Crank-Nicolson finite difference algorithm was used in place of a finite element algorithm. The typical heat-hold-cool processing cycle was assumed (Fig. 1). For purposes of this analysis, the processing system was assumed to be fixed. The length and diameter of the SSHE was constant at 1.829 m and 0.1523 m respectively, as was the length of the holding tube (60 m) (Table 1). All the other design and process/product specific parameters used in this evaluation are listed in Table 1 along with their assumed constant values and the range of values used for the simulation analysis.

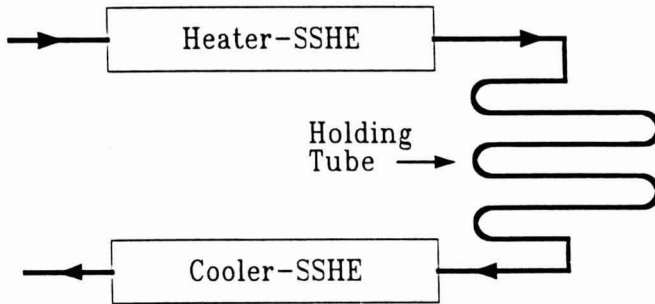


FIG. 1. HEAT-HOLD-COOL PROCESSING CYCLE ASSUMED FOR THE PROCESS SIMULATION

The values listed in Table 1 represent ranges for which the change in value was of interest. For example, the particle diameter, a parameter that would be controlled by the processor, was changed only from 0.02 to 0.022 m so that small changes in size could be investigated, and h_t was varied from 50 to 300 $W/m^2\text{ }^\circ C$ to reflect h_t values that would be characteristic of a stagnant layer of fluid surrounding the particle to that which represented a conservative estimate of h_t for a particle in flowing liquid. The constant values listed in Table 1 were used when the indicated parameter was held constant for the simulations. The constant thermal property values represent water for the fluid portion and beef for the particle portion (Sanz *et al.* 1987). The range of thermal property values used represents the low and high ends of the range of values assumed to be typical of food products processed in an aseptic system.

The determination of critical control factors of a process is dependent not only on whether the parameter influences the process, but also to what degree. Factorial designed analysis of a process allows one to take into account what is known about the system under study and determine comparisons, similarities,

TABLE 1.
DESIGN, PROCESS AND PRODUCT DEPENDENT VALUES
USED FOR THE SIMULATIONS

	Constant	Range
Design Specific Parameters		
Swept surface heat exchanger length	1.829m	-
Swept surface heat exchanger barrel diameter	0.1524m	-
Swept surface heat exchanger shaft diameter	0.0762m	-
Hold tube length	60m	-
Hold tube inside diameter	0.0475m	0.05-0.10m
Process Specific Parameters		
Hold tube surface temperature	25°C	20-30°C
Flow rate of product	0.2 kg/s	0.19-.21 kg/s
Particle diameter	0.02m	0.02-0.022m
Initial uniform product temperature	75 °C	65-85°C
Exit temperature of fluid from SSHE	140 °C	135-145°C
Product Specific Parameters		
SSHE overall surface heat transfer coefficient	2000 W/m ² °C	1000-4000 W/m ² °C
Hold tube overall surface heat transfer coefficient	0.0 W/m ² °C	0.0-20.0 W/m ² °C
Fluid-particle interface surface heat transfer coefficient in SSHE	800 W/m ² °C	500-1500 W/m ² °C
Fluid-particle interface surface heat transfer coefficient in hold tube	175 W/m ² °C	50-300 W/m ² °C
SSHE velocity ratio of particle	3.0	2.0-4.0
Hold tube velocity ratio of particle	2.0	1.8-2.2
Density of fluid	1000 kg/m ³	900-1100 kg/m ³
Specific heat of fluid	4187 J/kg°C	3000-4000 J/kg°C
Mass fraction of solids	0.25	0.10-0.50
Density of particle	1100 kg/m ³	1000-1200 kg/m ³
Specific heat of particle	3800 J/kg°C	3000-4000 J/kg°C
Thermal conductivity of particle	0.449 W/m°C	0.45-0.65 W/m°C

differences, and trends (Box and Draper 1987). Factorial experiments require at least two levels of analysis for each parameter. A two-level design is usually used for exploratory analysis of the variables with the minimum number of test runs. Considering the number of potential critical control factors that may possibly exist of an aseptic process of food products containing particulates, any analysis of the system will need to be done with as few test runs as possible. Simultaneous factorial analysis on 18 parameters would require completion of 262144 (2^{18}) simulations for a full two-level factorial design. An average of 14 seconds a run would take more than 42 days to complete on the computer equipment used for the analysis (MicroSoft FORTRAN 4.1 and a IBM PS/2 model 80). Thus, the analyses were broken into two groups of 13 parameters, eight of

the total 18 parameters being common between the two groups. Thus, instead of completing 262144 simulations 2×8192 (2×2^{13}) simulations were performed. The common parameters for the two groups were: (1) overall surface heat transfer coefficient for the SSHE (SSHE-U), (2) particle concentration (X), (3) maximum velocity ratio in the SSHE (VRH), (4) maximum velocity ratio in the holding tube (VRT), (5) particle diameter, (6) fluid-particle surface heat transfer coefficient in the SSHE (h_h), (7) fluid-particle surface heat transfer coefficient in the holding tube (h_t), and (8) product flow rate.

RESULTS AND DISCUSSION

The influence of a number of the parameters on the accumulated lethality (F_0 , $z = 10^\circ\text{C}$) of a process was primarily exponential. To linearize their influence as much as possible, the natural log of F_0 for the processes was regressed against the parameters. As an indication of the variations in F_0 and the steam requirements for changes in the investigated parameters, Table 2 lists the F_0 and heater steam temperature for simulations at the low and high end of each range for a given parameter when all the other parameters were at their constant values (Table 1). Tables 3 and 4 present the results of the regression analysis (i.e., coefficients and the resulting linear equation) for the two groups of parameters and the change in the parameter that would result in a 5.0 or 10.0% increase in the F_0 of the processes, as calculated from the regression equation. All the parameters were standardized (-1, 1) before they were regressed so that the coefficient of each parameter could be easily compared. This means that the coefficients of the parameters indicated in Tables 3 and 4 represent the change in the natural log of F_0 for a change in a parameter of half the range indicated in Table 1. For example, using the coefficients from the equation given in Table 3 it can be determined that a 0.001 m (1 mm) increase in the diameter of a particle (i.e., half the range of the parameter) will result in a decrease of F_0 for the processes of 0.96 min ($3.45 \cdot e^{1 \cdot 237 \cdot -0.323}$). The average F_0 for the first group simulation was 3.45 min (i.e., $e^{1 \cdot 237}$; 1.237 being the intercept for the equation).

All of the first order parameters for both groups except the fluid-specific heat parameter were significantly different from zero and thus, influenced the F_0 of the processes. Only a few of the second order variables were significant (Tables 3 and 4). For the first group, only one first order parameter, the surface air temperature for holding tube, was marginally significant as indicated by the coefficient being close to zero, primarily because the temperature differential between the temperature of the fluid in the holding tube and that of the surrounding air did not change appreciably with the change in air temperature. Thus, the heat transfer driving force did not change appreciably. The five predominant parameters influencing F_0 are exit temperature of the fluid from the heater, initial temperature, hold tube diameter, hold tube-U value, and h_i . The hold tube

TABLE 2.
ACCUMULATED PROCESS LETHALITY (min) AND HEATER STEAM TEMPERATURE (°C) FOR SIMULATIONS AT THE LOW AND HIGH END OF EACH PARAMETER RANGE WITH ALL OTHER PARAMETERS HELD AT THEIR CONSTANT VALUES

	Low		High	
	F ₀	Steam T.	F ₀	Steam T.
SSHE-U value	1.129	170.5	1.937	141.9
Mass fraction	1.666	148.9	1.087	149.0
Heater VR	2.521	148.6	1.056	148.6
Hold tube VR	2.731	148.6	0.781	148.6
Particle diameter	1.443	148.6	0.450	148.4
Particle heater-h value	1.110	148.5	1.829	148.7
Particle hold-h value	0.205	148.6	2.616	148.6
Product flow rate	2.130	147.8	0.970	149.5
Exit temp. of fluid	0.645	143.0	3.238	154.3
Hold tube air temp. ^a	0.717	148.6	0.760	148.6
Hold tube-U value	1.443	148.6	0.408	148.6
Hold tube diameter	2.621	148.6	287.3	148.6
Initial temp.	0.729	150.0	2.901	147.3
Density of fluid	0.754	148.6	2.435	148.7
Specific Heat of fluid	1.430	145.4	1.443	148.1
Density of particle	2.230	148.7	0.931	148.6
Specific heat of particle	6.692	147.9	0.999	148.8
Thermal cond. of particle	1.458	148.6	6.484	149.0

^a For hold tube-U value of 10.0 W/m²C

diameter is a design parameter and not a process/product-dependent variable, and a change in hold tube size of more than 0.6 mm would be needed to result in a 5% change in F₀, which is larger than the typical tolerance of polished stainless steel. Therefore, the significance of changes in the holding tube diameter over its entire length will be minor. However, it will have an influence on the fastest particle residence time, h_t, mass fraction, and particle diameter, as indicated by the interaction variables and in ways that cannot be determined by this computer simulation. As expected, the heating rate of the fluid (SSHE-U value, exit temperature of the fluid and initial temperature) is important in addition to the heat loss of the fluid in the holding tube to the surrounding air (hold tube-U value). The limited importance of SSHE-U is most probably a result of a fixed exit temperature of the fluid from the heater. As indicated by Lee *et al.* (1990), if the process controls the exit temperature of the fluid from the heater, the influence of SSHE-U on the F₀ of the processes is minimized. The hold tube-U value would best be minimized by insulating the holding tube, which is becoming an industry practice for the processing of food products containing particulates. No attempt was made to differentiate the air side h value, the fluid side h value, or the heat resistance of the wall itself with regards to the SSHE-U or hold tube U-value.

TABLE 3.
COEFFICIENTS OF REGRESSION ANALYSIS FOR NATURAL LOG OF F_0
AND CHANGE IN PARAMETER FROM ITS MEAN VALUE THAT RESULTS IN AN
INCREASE OF 5 AND 10% IN F_0 FOR FIRST SIMULATION
FOR SELECTED PARAMETERS USING A 2^{13} FACTORIAL DESIGN

Variable	Coefficient	5% Change In F_0	10% Change In F_0	Mean Value
<u>First Order Variables</u>				
SSHE-U value	0.276	265.	518.	2500. W/m ²⁰ C
Mass fraction (X)	-0.452	-0.022	-0.042	0.30
Heater VR (VRH)	-0.343	-0.142	-0.278	3.0
Hold tube VR (VRT)	-0.353	-0.028	-0.054	2.0
Particle diameter (PD)	-0.323	-0.00015	-0.00029	0.021 m
Particle heater-h value	0.238	102.	200.	1000. W/m ²⁰ C
Particle hold-h value	0.716	8.52	16.6	175. W/m ²⁰ C
Product flow rate	-0.239	-0.002	-0.004	0.20 kg/s
Exit temp. of fluid	0.796	0.306	0.599	140. °C
Hold tube air temp.	0.038	6.39	12.5	25. °C
Hold tube-U value (HU)	-1.16	-0.421	-0.822	10. W/m ²⁰ C
Hold tube diameter (HD)	1.98	0.0006	0.0012	0.075 m
Initial temp. (IT)	0.620	0.787	1.54	75. °C
Intercept	1.237			
<u>Important Second Order Variables</u>				
X*h _t	-0.141	-8.65	-16.9	52.5 W/m ²⁰ C
X*HD	-0.252	-0.001	-0.0019	0.0225m
VRH*h _t	0.133	45.9	89.7	525. W/m ²⁰ C
VRH*HD	0.188	0.0065	0.0127	0.225m
VRT*HD	0.126	0.0019	0.0038	0.15m
PD*HD	0.132	0.000009	0.000018	0.001575m ²
h _t *HD	-0.252	-0.605	-1.18	13.125 W/m ²⁰ C
h _t *IT	-0.129	-473.	-923.	13125. W/m ²
HU*HD	-0.588	-0.0207	-0.0405	0.75 W/m ²⁰ C
HD*IT	-0.226	-0.54	-1.05	5.625 m ²⁰ C

Coefficient of determination = 0.984

Total number of simulations was 8192 runs

Besides h_t the remaining first order parameters of the first group simulation are less significant in influencing the F_0 of the processes than the design parameters of hold tube diameter, hold tube-U value, exit temperature of the fluid from the heater, and initial temperature of the product. However, these parameters are very process/product-dependent and are not as easily controlled as most design parameters. A change in diameter of the particle of only 2 mm is more significant in changing the F_0 of the processes than a change in h_h from 500 to 1500 W/m²⁰C. This is also representative of the second group simulation (Table 4). The particle diameter is almost as influential as the fastest residence time factors for the heater and the holding tube (Tables 3 and 4). Therefore, the

TABLE 4.
COEFFICIENTS OF REGRESSION ANALYSIS FOR NATURAL LOG OF F_0 AND CHANGE
IN PARAMETER FROM ITS MEAN VALUE THAT RESULTS IN AN INCREASE OF
5 AND 10% IN F_0 FOR FIRST SIMULATION FOR SECOND SIMULATION
FOR SELECTED PARAMETERS USING A 2^{13} FACTORIAL DESIGN

Variable	Coefficient	5% Change In F_0	10% Change In F_0	Mean Value
<u>First Order Variables</u>				
SSHE-U value	0.329	222.	434.	2500. W/m ² °C
Mass fraction	-0.144	-0.068	-0.133	0.30
Heater VR	-0.537	-0.091	-0.177	3.0
Hold tube VR	-0.475	-0.021	-0.040	2.0
Particle diameter	-0.446	-0.0001	-0.00021	0.021m
Particle heater-h value	0.327	74.7	146.	1000. W/m ² °C
Particle hold-h value	1.143	5.34	10.4	175. W/m ² °C
Product flow rate	-0.347	-0.0014	-0.0027	0.20 kg/s
Density of fluid (D_f)	0.475	10.26	20.1	1000. kg/m ³
Specific Heat of fluid	-0.006	-4440	-8670	3500. J/kg°°C
Density of particle	-0.337	-14.5	-28.2	1100. kg/m ³
Specific heat of particle	-0.854	-28.6	-55.8	3500. J/kg°°C
Thermal cond. of particle	0.698	0.007	0.0137	0.55 W/m°°C
Intercept	0.538			
<u>Important Second Order Variables</u>				
$X \cdot h_t$	-0.194	-6.29	-12.3	52.5 W/m ² °C
$X \cdot D_f$	-0.140	-6.97	-13.6	300. kg/m ³
$VRH \cdot h_t$	0.226	27.0	52.7	525. W/m ² °C

Coefficient of determination = 0.979

Total number of simulations was 8192 runs

maintenance of the maximum particle size is critical in ensuring the safety of an aseptic process.

Because these analyses are for unidirectional heat transfer and most particulates processed aseptically will result in three- if not two-dimensional heat transfer, the need to control all the dimensions of a multidimensional particle is still under investigation. This investigation must include what would occur if a three-dimensional particle were controlled only on two dimensions because of the difficulty in developing process control procedures to control three dimensions; two dimensions would not be that difficult. Chandarana and Gavin (1989b) have investigated this problem and have shown that the loss of one dimension may result in more than a four-fold change in the F_0 of the processes. However, research into this topic needs to continue.

Of the process/product-dependent parameters, h_t was the most influential in changing the value of F_0 for the processes (Table 3 and 4) because of the low

TABLE 5.
COEFFICIENTS OF REGRESSION ANALYSIS FOR NATURAL LOG OF F_0 AND CHANGE IN PARAMETER FROM ITS MEAN VALUE THAT RESULTS IN AN INCREASE OF 5 AND 10% IN F_0 FOR THREE AND FIVE FACTORIAL LEVEL SIMULATION OF SELECTED PARAMETERS

Variable	Coefficient	5% Change In F_0	10% Change In F_0	Mean Value
<u>First Order Variables</u>				
Heater VR ^a	-0.453	-0.108	-0.211	3.0
Hold tube VR ^a	-0.483	-0.02	-0.039	2.0
Particle hold-h value ^b	1.18	5.18	10.1	175. W/m ² °C
Density of fluid ^a	0.491	9.93	19.4	1000. kg/m ³
Specific Heat of fluid ^a	-0.0097	-2500	-4900	3500. J/kg°C
Density of particle ^a	-0.352	-13.9	-27.1	1100. kg/m ³
Specific heat of particle ^b	-0.829	-29.4	-57.5	3500. J/kg°C
Thermal cond. of particle ^b	0.662	0.0074	0.0144	0.55 W/m°C
Intercept	1.405			
<u>Important Second Order Variables</u>				
h_t^2	-0.712	-1070	-2090	30625. W ² /m ⁴ °C ²
Coefficient of determination = 0.975				
Total number of simulations was 30375 runs				

^a Three levels used for simulation of parameter.

^b Five levels used for simulation of parameter.

values used in the simulation for h_t . For processes where the h_t values are between 50 and 300 W/m²°C, small changes will greatly influence the F_0 of the processes. A change of h_t of only 6 W/m²°C (175 to 181 W/m²°C) results in more than a 5% increase in F_0 (Table 3). Thus, considerable process control must be implemented to prevent h_t from falling below its design level. Besides h_t the residence time of the fastest particle in both the heater and the hold tube proved to be the most influential.

Previous research has consistently indicated that the residence time of the fastest particle is very important in determining the minimum processing time of a product (Sastry 1986; Chandarana and Gavin 1989b; Lee *et al.* 1990). Some work has been done to determine if the largest particle of a food product that contains various particle sizes would travel fastest. McCoy *et al.* (1987) showed that for individual particles (i.e., no particle-to-particle interactions) the residence time depends on particle size, and the slowest is not necessarily the largest. Berry (1989) demonstrated that the residence time of particles depends on the size of the particles in the product, the larger particle primarily influencing the flow behavior of the smaller. He also observed that the smallest particle

was routinely the fastest and never faster than twice the average bulk flow rate. Berry (1989) points out, however, that this analysis was for a model system and that the results may not be applicable to real foods. A conservative approach to process establishment would be to assume that the largest and fastest particle travels at twice the average flow rate. Otherwise, detailed data must be measured to develop a basis for the particle that receives the smallest accumulated lethality when it is other than the fastest and largest.

The simulation for the second group of parameters included thermal properties for both the fluid and particulates of the food product. For the range tested the specific heat and thermal conductivity of the particle were almost as influential as h_t in changing the F_0 of the processes. The coefficient for the direct effect of the fluid specific heat parameter was not statistically different from zero and thus, does not significantly influence the accumulated lethality of the process. The specific heat of the fluid will, however, influence h_h , h_t and the SSHE U-value in ways that could not be determined using this computer simulation.

Very little work has been done on measuring thermal properties of particulates and on any changes in the thermal properties that may result during the processing of the food product. Kravets and Diehl (1989) have presented a procedure to measure the thermal conductivity of small particulate items that can be used at aseptic processing temperatures. Considering the importance of the thermal properties of fluid and particulates and the lack of any research in this area, work in this area should be initiated.

The change in flow rate in its range of low to high results in a 30.5 s decrease in processing time (307s) for the heater and hold tube sections. This explains the importance of this parameter on F_0 of just less than 5% (Table 3). This corresponds to a product flow rate control of almost three significant figures or a maximum fluctuation of only ± 0.001 Kg/s for the flow rate used in this study. Since the possibility of controlling the flow rate to this precision is unlikely, the flow rate of the product must be controlled to such a degree below the design rate so that maximum deviation of the flow rate cannot exceed it.

The magnitude of the coefficient for the mass fraction parameter is small for the second group simulation. This implies that for small variations of particulate concentration (i.e., those that would normally occur within the heater and hold tube during processing) the F_0 of the processes may not be significantly influenced.

A final factorial design simulation was completed for a limited number of some of the more influential process/product-dependent parameters (Table 5). This simulation was conducted at three and five levels so that a more complete understanding of the significance of each of the variables could be obtained. The results are almost identical to those obtained in Table 4. Thus, for this model the two level factorial design results are adequate in describing the influence of each parameter on the F_0 of the processes. The additional simulation, however,

allowed for the testing of the nonlinear nature of each parameter (i.e., square of parameter) for which h_t^2 proved to be significant. This indicates that h_t does not influence F_0 on an exponential nature but more on a linear relationship, which agrees with the data obtained by Chandarana *et al.* (1989).

Mathematical modeling such as this aids the food processing industry in developing better process control and in understanding the parameters associated with a system's design. However, in the case of aseptic processing of low-acid food products containing particulates, the development of a conservative process design is a mixture of mathematical modeling experimental results, and biological measurements, with the actual verification of the process conducted biologically (Dignan *et al.* 1989).

REFERENCES

- BERRY, M.R. 1989. Predicting fastest particle residence time. In *Proceeding of the First International Congress on Aseptic Processing Technologies*, (J.V. Chambers, ed.) pp. 6-17, Food Science Dept., Purdue University, W. Lafayette, IN.
- BOX, G.P. and DRAPER, N.R. 1987. *Empirical Model-Building and Response Surfaces*. pp. 105-135, John Wiley & Sons, New York.
- CASTAIGNE, F. and LACROIX, C. 1987. Calculation of residence times for the sterilization of low acid liquid foods containing particulates in continuous aseptic packaging process. Presented at the Canadian Engineering Centennial Convention of the CSAE, Montreal, P.Q., May 18-22. Paper No. 87505.
- CHANDARANA, D.I., GAVIN, III., A. and WHEATON, F.W. 1989. Simulation of parameters for modeling aseptic processing of foods containing particulates. *Food Technol.* 43(3), 137-143.
- CHANDARANA, D.I. and GAVIN, III, A. 1989a. Establishing thermal processes for heterogeneous foods to be processed aseptically: a theoretical comparison of process development methods. *J. Food Sci.* 54, 198-204.
- CHANDARANA, D.I. and GAVIN, III, A. 1989b. Modeling and heat transfer study of heterogeneous foods processed aseptically. In *Proceeding of the First International Congress of Aseptic Processing Technologies*, (J.V. Chambers, ed.) pp. 56-86, Food Science Dept., Purdue University, W. Lafayette, IN.
- de RUYTER, P.W. and BRUNET, R. 1973. Estimation of process conditions for continuous sterilization of foods containing particulates. *Food Technol.* 27(7), 44-51.
- DIGNAN, D.M., BERRY, M.R., PFLUG, I.J. and GARDINE, T.D. 1989. Safety considerations in establishing aseptic processes for low-acid foods containing particulates. *Food Technol.* 43(3), 118-121, 131.

- KRAVETS, R.R. and DIEHL, K.C. 1989. Method for measurement of thermal conductivity of small food particulates at thermal processing temperature. Presented at Annual IFT meeting. Chicago, IL., June 25-29. Paper No. 557.
- LARKIN, J.W. 1989. Use of a modified Ball formula method to evaluate aseptic processing of foods containing particulates. *Food Technol.* 43(3), 124-131.
- LEE, J.H., SINGH, R.K. and LARKIN, J.W. 1990. Determination of lethality and processing time in a continuous sterilization system containing particulates. *J. Food Eng.* 11, 67-92.
- MANSON, J.E. and CULLEN, J.F. 1974. Thermal process simulation for aseptic processing of foods containing discrete particulate matter. *J. Food Sci.* 39, 1084-1089.
- McCOY, S.C., ZURITZ, C.A. and SASTRY, S.K. 1987. Residence time distributions of simulated food particles in a holding tube. Presented at the International Winter Meeting of the ASAE, Chicago, IL., December 15-18. Paper No. 87-6536.
- SANZ, P.D., ALONSO, M.D. and MASCHERONI, R.H. 1987. Thermophysical properties of meat products: General bibliography and experimental values. *Trans. of ASAE.* 30, 283-296.
- SASTRY, S.K. 1986. Mathematical evaluation of process schedules for aseptic processing of low-acid foods containing discrete particulates. *J. Food Sci.* 51, 1323-1328, 1332.
- SASTRY, S.K. 1988. Process evaluation in aseptic processing. In *Developments in Food Preservation*, Vol. 5, (S. Thorne, ed.) pp. 177-206, Elsevier Applied Sci. Publ. Essex, England.

CHANGES IN PARTITION COEFFICIENTS OF ALCOHOLS AS AFFECTED BY THE PRESENCE OF VARIOUS FOOD SOLIDS

SEESUB CHUNG and RICARDO VILLOTA¹

*Department of Food Science
University of Illinois
Urbana, Illinois*

Accepted for Publication July 24, 1990

ABSTRACT

Using homologous series of alcohols and varying temperatures, it has been demonstrated in this study that volatility of alcohols increases upon changes in the system which decrease their solubility in the liquid. Addition of solutes has various effects on volatility, depending upon their ability to interact with water and volatiles. Surface characteristics, including the number of binding sites and surface area, significantly affect interaction. When more than one type of solids is present, alcohols preferentially adsorb to the solid with higher affinity for alcohols, until all binding sites on the solid are occupied. Silica and soy protein increase solubility of alcohols in water by adsorbing them through hydrophobic association and/or hydrogen bonds. Sodium silicoaluminate, xanthan gum and, to some extent, maltodextrin show less interaction with alcohols than with water.

INTRODUCTION

Flavoring substances are important constituents of food materials, even though their total content in food is very small, usually ranging between 1 and 1000 mg/kg of food (Maier 1970). The perceived flavor has a large influence on selection and acceptance of foods by consumers. The flavor of a food is characterized by volatile compounds in the atmosphere above the food. The concentration of a volatile compound in the headspace is determined by its air-liquid partition coefficient (K_{al}).

It has been reported that air-water partition coefficients (K_{aw}) of volatile compounds in a dilute water solution gradually increase with an increasing molecular weight of the compounds in a homologous series (Butler *et al.* 1935; Buttery *et al.* 1965, 1971; Kieckbusch and King 1979). The coefficients are, however, relatively independent of the concentration of volatiles as long as they are present below the saturation level (Buttery *et al.* 1969).

¹Correspondence to: Dr. R. Villota, University of Illinois, Department of Food Science, 382D Agric. Eng. Sci. Bldg., 1304 W. Pennsylvania Ave., Urbana, Illinois 60801.

When there is a nonvolatile third component in a food system, this coefficient is called air-liquid partition coefficient to distinguish it from the one for a two-component system. The presence of nonvolatile solutes in a system will change the concentration of volatile in a vapor phase by interacting with the volatile components. Therefore, the binding of flavor compounds by food components can be examined by comparing the air-liquid partition coefficients with the air-water partition coefficients.

It has been known that the addition of inorganic salts increases vapor pressure of volatile components in dilute aqueous solutions (Jennings 1965; Nelson and Hoff 1968). This phenomenon has been used for the gas chromatographic analysis of vapor concentration (Vitenberg *et al.* 1974).

Carbohydrates have shown rather complex effects on volatile concentration in the headspace. Sucrose, for instance, increased the volatility of acetone in an aqueous solution, whereas it decreased the volatilities of 2-heptanone and heptanal (Nawar 1971). According to the author, the decrease in headspace concentration upon the addition of sucrose to aqueous volatile solutions does not involve a direct interaction between sugar and volatiles, but rather it occurs via interaction of the sugar with water molecules. Many other researchers have also reported similar effects of carbohydrates on volatilities of various organic compounds in dilute aqueous solutions (Wientjes 1968; Voilley and Richon 1986; Kieckbusch and King 1979; Lebert and Richon 1984).

Proteins also have variable influence on headspace concentrations of volatile compounds. Nawar (1971) showed decreased concentrations of ketones in the headspace with the addition of gelatin to water containing the volatiles. The author, however, found that the order of addition of ingredients greatly affected the results. When the volatiles were added to gelatin solutions, the headspace concentrations of the ketones increased. Franzen and Kinsella (1974) found that the addition of various food proteins to water-soluble systems decreased the concentration of volatiles in a headspace by aiding solubilization of volatiles.

Amorphous silicas are widely used in food processing to provide various functional properties, one of which is adsorption. The interaction of amorphous silica with organic molecules is strongly affected by the degree of hydroxylation of the surface. A fully hydroxylated surface is completely hydrophilic, whereas the siloxane surface is essentially hydrophobic. Iler (1979) noted that a maximum adsorption of polar molecules would occur when the silica surface is free of adsorbed water and has a maximum concentration of silanol groups. It is known that many physically adsorbed molecules form hydrogen bonds with surface hydroxyl groups (Curthoys *et al.* 1974).

There has been a considerable amount of work devoted to the area of measuring changes of volatilities due to adsorption of flavor compounds by food solids in solution. However, the subject is poorly understood, and thus it is still difficult to predict how volatile molecules behave in the presence of nonvolatile

solutes. The choice of flavor-fixing materials becomes very important since flavor compounds interact with food components in varying degrees. Better knowledge of the flavor-solid interactions and techniques to control them will enable one to overcome evaporative losses of flavor and lead to the development of better flavored products. It is, therefore, within the scope of this investigation to determine differences in mechanisms of flavor binding by different types of food solids and to examine the possibility of using fumed silica as a flavor carrier.

TABLE 1.
PHYSICAL PROPERTIES OF VARIOUS SILICAS

COMMERCIAL NAMES	CLASSIFICATION	SPECIFIC GRAVITY	BULK DENSITY (lb/ft ³)	PARTICLE SIZE (nm)	SURFACE AREA (m ² /g)
Cab-O-Sil EH-5 (Cabot Corp., Tuscola, IL)	fumed silica	2.2	2.3	7	330
Aerosil 200 (Degussa Corp., Teterboro, NJ)	fumed silica	2.2	3.1	12	180
Hi-Sil T600 (PPG Industries, Pittsburg, PA)	precipitated	2.1	3 - 4	21	120
Zeolex 23A (J.M. Huber Corp., Havre de Grace, MD)	sodium silicoaluminate	2.1	16 - 18	6000	45

MATERIALS AND METHODS

Materials

Alcohols have been chosen as model flavor compounds for this investigation. Alcohols, besides being present in a wide range of foods, possess mixed hydrophobic and hydrophilic character. The headspace of the homologous series of the aliphatic alcohols, from methanol to butanol, in the presence of food powders was analyzed.

Food powders selected for this research were soy protein isolate, xanthan gum, maltodextrin and silicon dioxide. Various types of silica were tested for their adsorption characteristics. Silicas have different surface properties depending upon the method used in their production. Table 1 lists the physical properties of the silica powders used in this research. Soy proteins, which are widely used in the manufacture of fabricated foods, have been known to interact with various flavor compounds. Due to the short supply and high price of gums, it has

become necessary to search for replacements. In accordance with preliminary research data, Cab-O-Sil, a fumed silica, has been chosen as a possible replacement for gums and tested for its ability to aid flavor retention.

Methods

For the determination of air-water partition coefficients, about one-third of a flask was filled with water, and then a certain amount of a volatile compound was added to the water. After shaking for thorough mixing, the flask was allowed to stand for at least 18 h to reach equilibrium in a water bath maintained at a desired temperature. Preliminary tests showed that equilibration of n-butanol was reached in less than 10 h at 20 °C. At the end of the equilibration period, known amounts of vapor samples (2 mL) and liquid samples (2 μ L) were alternately injected into a gas chromatograph. The syringe for vapor sampling was gas-tight and water-jacketed to prevent condensation of the volatile compounds on the syringe wall. The temperature of the water circulating around the syringe was set at 2 °C higher than the temperature for equilibration of the sample. Syringes were flushed three times before taking a required amount of sample.

Ternary systems of water-solid-volatile were prepared by mixing the solids with water in a flask before the addition of volatile compounds. For the headspace analysis of volatiles in systems containing nonvolatile solutes, 2 mL of vapor samples were injected into a gas chromatograph after the same treatment as for the determination of K_{aw}

Due to the presence of nonvolatile solutes in the liquid phase, it was impossible to inject liquid samples into a gas chromatograph. Therefore, an indirect method, developed by Kieckbush and King (1979), was used to determine the partition coefficient of volatile compounds in solutions containing solids. This method is based on an equation derived from a mass balance between the vapor and liquid phases, which can be expressed as:

$$K_{al} = K_{aw} (m_w/m_1) (R_1/R_w) (V_1/V_w) \quad (1)$$

where m_w , m_1 = mass of a volatile component in secondary system and ternary system, respectively

R_w , R_1 = chromatographic response of vapor samples from secondary system and ternary system, respectively

V_w , V_1 = volume of water in secondary system and of liquid in ternary system, respectively.

Since K_{aw} is easily measured, K_{al} can be calculated if R_1/R_w is determined by gas chromatographic analysis of the headspace vapor.

There is, however, a limitation in examining partition coefficients for interactions between volatiles and food components since it requires a liquid system. For pasty or dry systems, the difference in headspace concentration of volatiles

was measured between the system with and without the food powder. This difference indicates the reactivity of volatiles with the solid components. The control samples contained glass beads instead of the food powder to compensate a reduction in the volume of the headspace by the food powder. The volumes occupied by solids were estimated from their true densities and ranged from 1.3 to 1.9 cm³. The density was measured by placing a certain amount of powder into a graduated cylinder which was then compacted with a plunger until no volume change was observed. Similar sampling and analytical procedures were used as described for the determination of partition coefficients.

The gas chromatograph used in this research was an HP-5739A equipped with a dual flame ionization detector and an HP-3390A integrator. Glass columns (6 ft × 1/4 in. OD) were packed with Porapak Q for analysis of methanol and ethanol, or with 10% Carbowax 20M on 80/100 Chromosorb W AW for higher alcohols than ethanol. Flow rates of carrier gas (nitrogen) and hydrogen were 40 mL/min, and air flowed at the rate of 250 mL/min. Temperatures of oven, injection port and detector were varied depending on the compounds of interest to have faster analysis.

RESULTS AND DISCUSSION

Table 2 lists the air-water partition coefficients of aliphatic alcohols (C1 to C4) determined in the present work, and for comparison, those reported in the literature. Values of Butler *et al.* (1935) were calculated from their reported values of P/N where P is the partial pressure of the volatile solute and N is the molar fraction of the volatile in solution. From the results in this table, it is obvious that partition coefficients of normal alcohols in aqueous solutions increase with their molecular weight. This may result from the decreased solubility of alcohols due to increased repulsive forces between water and alcohol molecules as the chain length of alcohols increases. By the same token, a branched alcohol (2-propanol) shows a higher partition coefficient than its unbranched counterpart (1-propanol). Branching will prevent molecules from approximating each other or to water molecules for the formation of hydrogen bonding.

It also can be seen in this table that the air-water partition coefficients at 25 °C are significantly higher than those at 20 °C. The dependency of the partition coefficients on temperature is illustrated for ethanol in Fig. 1. The relationship can be expressed by the equation:

$$\ln K_{aw} = (\Delta H_v/RT) + \text{const} \quad (2)$$

where T = absolute equilibrium temperature

R = gas constant

ΔH_v = heat of vaporization.

TABLE 2.
AIR-WATER PARTITION COEFFICIENTS OF ALIPHATIC ALCOHOLS

ALCOHOL	AIR-WATER PARTITION COEFFICIENT ($\times 10^{-4}$)			
	Present Work		Butler et al. (1935)	Mazza (1980)
	20°C	25°C	25°C	25°C
methanol	0.96 ± 0.01	1.29 ± 0.02	1.79	0.03
ethanol	1.08 ± 0.06	1.42 ± 0.02	2.12	0.65
n-propanol	1.46 ± 0.01	2.10 ± 0.12	2.82	1.08
iso-propanol	2.06 ± 0.03		3.29	1.96
n-butanol	1.70 ± 0.03	2.73 ± 0.04	3.49	

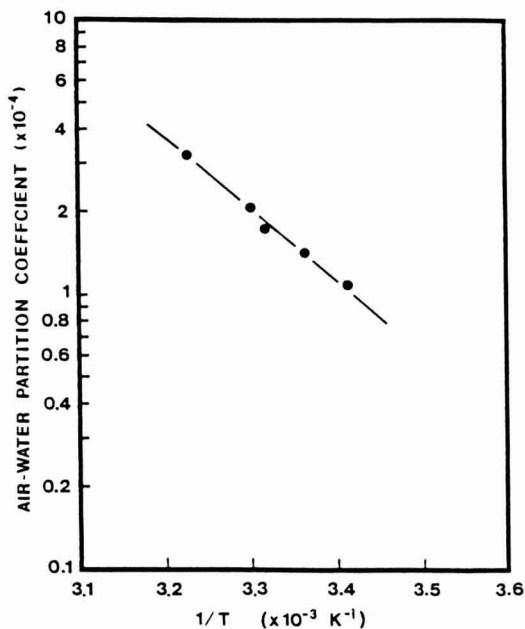


FIG. 1. VARIATION OF AIR-WATER PARTITION COEFFICIENTS OF ETHANOL WITH TEMPERATURE

Therefore, plots of K_{aw} vs $1/T$ fall close to a straight line with a slope related to the heat of vaporization. In the case of ethanol, the calculated ΔH_v was 11.6 kcal/mol, somewhat higher than the latent heat of vaporization of pure ethanol which would be 9.8 kcal/mol at 28 °C. The heat of vaporization reflects the strength of molecular interactions, thus the higher heat of vaporization for

ethanol in water seems reasonable since interactions of ethanol with water molecules, which have higher polarity, are stronger than interactions among ethanol molecules. This calculated value is generally within the range reported by other researchers.

Nonvolatile solutes can adsorb volatile solutes to binding sites on the surface. In ternary systems containing water, nonvolatile solutes and volatile compounds, the interactions among the three components can be examined by analyzing the concentration in the headspace vapor in equilibrium with the liquid phase. As a result of the interactions, there will be changes in the air-liquid partition coefficient, and the magnitude of the change can be expressed as the ratio of the headspace concentrations of a volatile in a ternary system to that in a water-volatile system (R_1/R_w).

Table 3 lists the changes in headspace concentrations of 1-propanol and 1-butanol at various concentrations upon the addition of solids at the 2% level. This low content of solids is essential to apply Eq. (1) to determine K_{al} .

TABLE 3.
CHANGES IN VAPOR CONCENTRATION OF 1-PROPANOL AND 1-BUTANOL
DUE TO THE PRESENCE OF FOOD POWDERS (25°C)

ALCOHOL CONC. (ppm)	K_{aw} ($\times 10^{-4}$)	R_1/R_w		
		Silica	Soy Isolate	Xanthan Gum
1-Propanol				
1000	2.10 ± 0.12	0.76 ± 0.03	0.95 ± 0.01	1.05 ± 0.04
1500	2.11 ± 0.06	0.88 ± 0.13	0.96 ± 0.01	0.99 ± 0.01
2000	1.96 ± 0.07	0.90 ± 0.01	0.97 ± 0.01	1.04 ± 0.03
2500	2.12 ± 0.09	0.91 ± 0.01	0.94 ± 0.03	1.07 ± 0.05
1-Butanol				
1000	2.54 ± 0.14	0.78 ± 0.05	0.97 ± 0.04	1.09 ± 0.01
1500	2.71 ± 0.05	0.85 ± 0.01	0.96 ± 0.03	1.05 ± 0.02
2000	2.73 ± 0.10	0.89 ± 0.04	0.97 ± 0.02	1.03 ± 0.01
2500	2.65 ± 0.07	0.90 ± 0.05	0.96 ± 0.02	0.99 ± 0.01

The values of K_{aw} and R_1/R_w are the averages of triplicates and their standard deviations.

While partition coefficients of volatiles between air and liquid phases are generally independent of solute concentration as long as the volatile concentration is low enough, the partition coefficients between a solid phase and a liquid

phase tend to be very sensitive to volatile concentration (King 1974) as in the case of silica. The fraction adsorbed onto the silica surface, for a given ratio of solid surface area to volume of water, will be higher at lower volatile concentrations. While the silica has shown better ability to decrease volatilities of both alcohols, soy isolate and xanthan gum do not change vapor pressure significantly, possibly due to a high molar ratio of alcohols to solids. These differences are reasoned as results of the different capability of solids to interact with water or alcohols. According to King (1983), there can be two conflicting effects affecting this capacity: (1) intermolecular interactions between alcohols and solids, which suppress volatilities of alcohols, and (2) salting-out effects from the solids interacting with water, which increase volatilities. Therefore, which one of these two effects becomes dominant in a given system will depend on the surface properties of the solid in the system.

The effects of water content on interactions between alcohols and solids were studied with a system in which the amount of water was fixed at 1 mL and the amount of powder was varied. Another system had varying amounts of water and a constant weight of powder. Although Eq. (1) is no longer applicable at high solids contents, it is felt that studies on headspace concentrations of volatile components for various compositions of solids and water can provide information on the interactions between powders and volatiles.

Shown in Fig. 2 is the experimental data of R_1/R_w when the amount of water was fixed at 1 mL while changing the amount of solutes. Cab-O-Sil shows a great ability to adsorb ethanol molecules, decreasing the vapor concentration of ethanol by about 60% when the solid content is 50%. With soy protein isolate, there is a very small decrease in the vapor concentration of ethanol. This decrease in the presence of silica or protein may result from intermolecular interactions between solids and volatiles. The ethanol content in the headspace, on the other hand, greatly increases in the presence of xanthan gum. This is mostly due to adsorption of water to gum molecules which increases the mole fraction of ethanol in the liquid phase.

Changes in R_1/R_w of n-alcohols (C1 to C4) were also studied by adding various amounts of water to a fixed amount of powder. Differences in the behavior of alcohols with different types of solids may be attributed to their capabilities to interact with water and alcohols. Changes in headspace concentration depend upon the interactions of solids not only with alcohols but also with water.

There are at least two possible mechanisms regarding the effect of water on the vapor pressure of volatiles. As the amount of water increases, more alcohol will be solubilized, resulting in less alcohol in the vapor phase. On the other hand, water molecules may compete with alcohol molecules for binding sites on solids. Therefore, the number of binding sites and the amount of water will

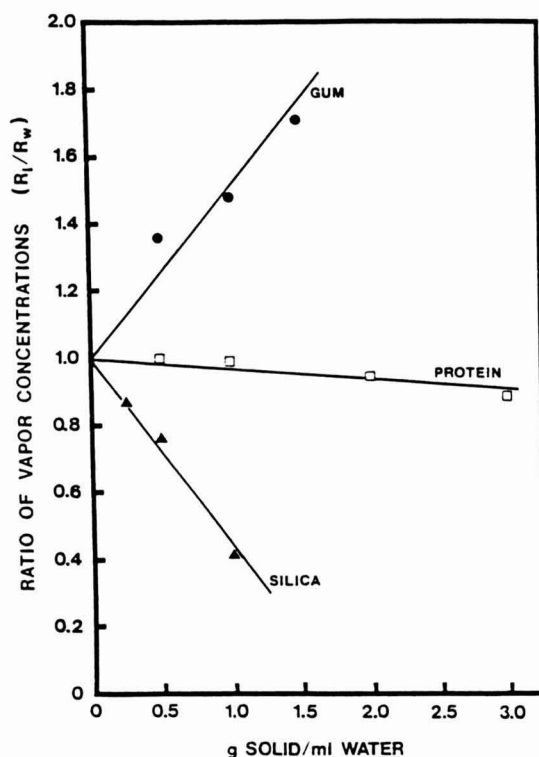


FIG. 2. EFFECT OF SOLID CONTENT ON VAPOR CONCENTRATION OF ETHANOL

determine which of these effects becomes dominant. At high water contents, alcohol molecules may compete with water for binding sites on the silica (Fig. 3). Therefore, the degree of reduction in concentrations of alcohols in the headspace by the silica continuously becomes greater as the Cab-O-Sil content increases. Cab-O-Sil has a large number of hydroxyl groups on the surface which are capable of forming hydrogen bonding with a variety of volatile compounds. This fact, coupled with a large surface area of the silica, may result in a continuous decrease in vapor concentration of all alcohols tested with an increase in solids content.

Figure 3 also shows a larger drop in the vapor concentration of alcohols as their chain length increases in the presence of silica. The water solubility of organic compounds within a homologous series decreases with an increase in their molecular weight. According to Weber (1985), the greater the solubility of a compound, the smaller the extent of adsorption of the compound from a solvent, and the stronger the bond between an adsorbate and a solvent. The bond must be broken before adsorption occurs. As a result, adsorption from an

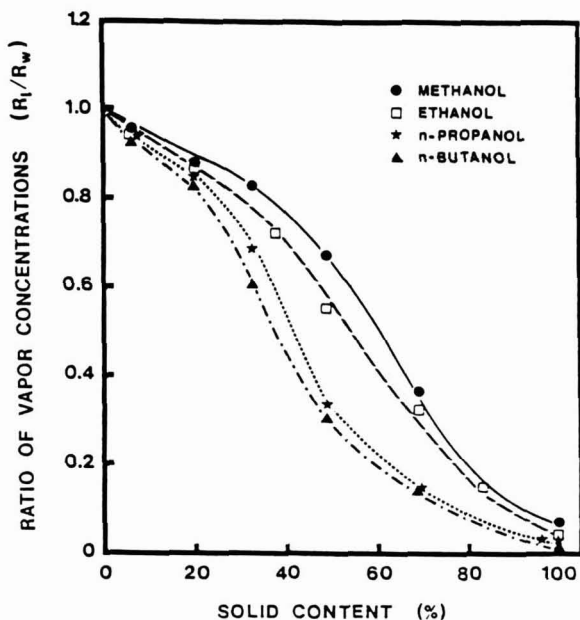


FIG. 3. CHANGES IN VAPOR CONCENTRATION OF ALCOHOLS AS A FUNCTION OF SILICA CONTENT

aqueous solution increases as a homologous series is ascended, largely because the expulsion of increasingly larger hydrophobic molecules from water results in an increasing number of water-water bonds and less water-adsorbate bonds.

Different methods of manufacturing silica powders result in various types of silica surfaces. It has been of interest to investigate how adsorption is affected by the differences in surface characteristics. Figures 4 and 5 show changes in vapor concentrations of ethanol and 1-butanol by various types of silica. Cab-O-Sil interacts most with these alcohols, while Zeolex shows little interaction. The differences in adsorption are mostly due to the differences in surface areas and properties of the silicas.

Fumed silicas such as Cab-O-Sil EH-5 and Aerosil 200 have a very large surface area, and a high concentration of isolated silanol groups. Alcohols may form hydrogen bonds with these sites and are further stabilized by hydrophobic interactions. These characteristics of fumed silica result in a large reduction of vapor concentration of alcohols for the whole range of silica contents. A slightly higher adsorption of alcohols to Cab-O-Sil than Aerosil is related to the larger surface area of Cab-O-Sil.

Precipitated silica, Hi-Sil T600, has a considerably smaller surface area. The surface of this type of silica is saturated with silanol groups which are hydrogen-bonded with water molecules. The bound water molecules are in turn coated

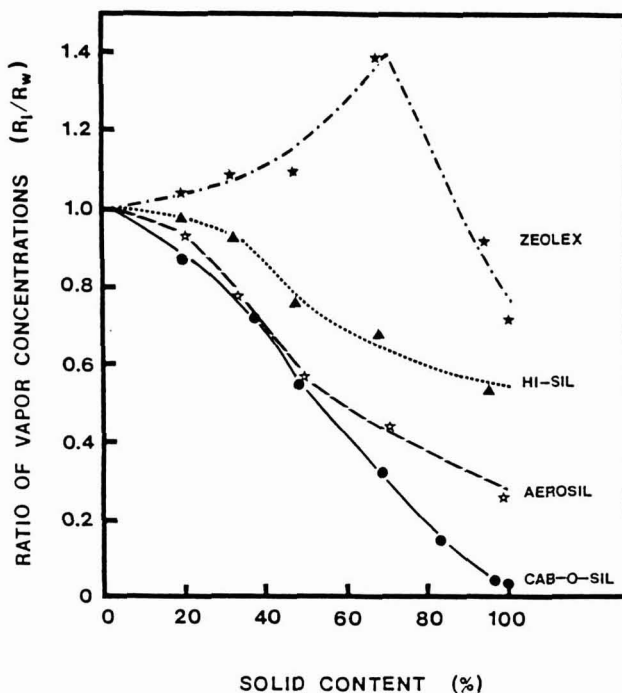


FIG. 4. CHANGES IN VAPOR CONCENTRATION OF ETHANOL AS A FUNCTION OF THE TYPE OF SILICA

with free water molecules, thus showing a strongly hydrophilic nature. However, the hydrogen-bonded silanol groups have very little tendency to form hydrogen bonds except with strong electron donor atoms such as water and methanol. Thus only small amounts of alcohols will be adsorbed from the water phase on precipitated silica.

Adsorption of alcohols to sodium silicoaluminate, Zeolex 23A, is mostly governed by interactions between water and the silica because the silica exerts little ability to interact with ethanol and n-butanol molecules. Therefore, the adsorption of water to the silica will increase vapor concentration of alcohols due to expulsion of alcohol molecules from the water phase. After a maximum increase at around 70% solid content, the ratio of vapor concentrations of alcohols in the headspace above Zeolex solutions to those of control samples decreases, possibly due to the fact that adsorption sites become available for alcohol molecules as there is less water in the system.

Comparing Figs. 4 and 5, 1-butanol is adsorbed more on fumed silica than ethanol. Since butanol forms weaker hydrogen bonds with water than ethanol does, it is easier for butanol to be adsorbed to the fumed silica. It would be

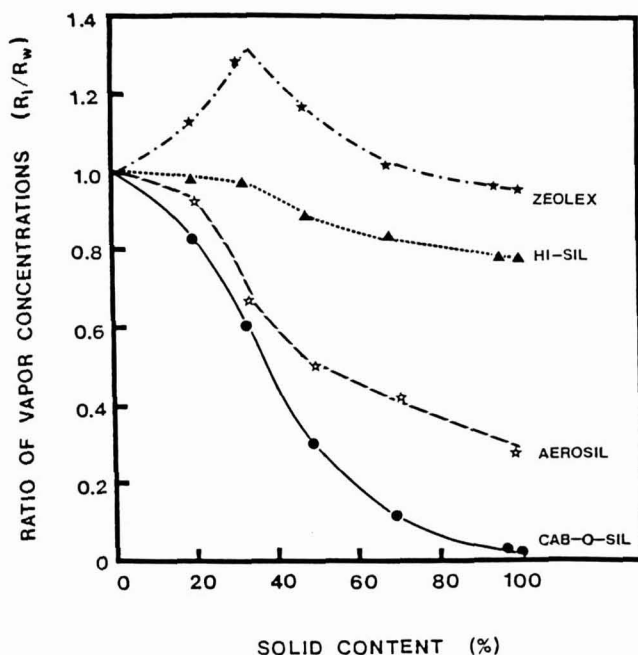


FIG. 5. CHANGES IN VAPOR CONCENTRATION OF N-BUTANOL AS A FUNCTION OF THE TYPE OF SILICA

reasonable to assume that the adsorption of butanol molecules to the silica is mostly a result of hydrophobic interactions between siloxane groups and methyl ends on butanol molecules, because water molecules may occupy the majority of the hydrophilic sites. In the case of Hi-Sil, less extent of adsorption occurs with butanol than with ethanol. This is due to the fact that silanol groups on the fully hydroxylated Hi-Sil surface are hydrogen-bonded, and that butanol has a weaker tendency to form hydrogen bonds than ethanol. Due to the lower solubility of butanol in water, the maximum increase in the vapor concentration of 1-butanol by the presence of Zeolex occurs at a lower solid content, compared to changes in concentration of ethanol vapor.

The vapor concentration of alcohols shows a complex behavior in a system with xanthan gum (Fig. 6). The gum initially increases the vapor pressure of alcohols as its content increases. At a solids content around 60 to 70%, the headspace concentration of alcohols starts to decrease. After reaching a minimum, the alcohol content in a vapor phase rises again as the gum becomes drier, except for methanol whose concentration remains relatively constant when the gum content is between 90 to 100%.

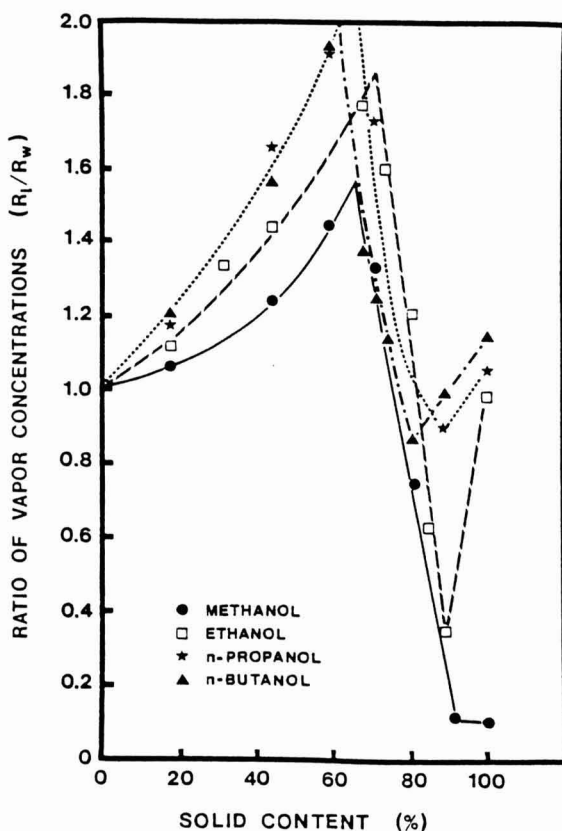


FIG. 6. CHANGES IN VAPOR CONCENTRATION OF ALCOHOLS AS A FUNCTION OF XANTHAN GUM CONTENT

Xanthan gum, the best adsorbent of water among the studied powders, increases vapor pressure of alcohols when water molecules occupy binding sites so that less amount of water is available to solubilize alcohols. The increase in vapor pressure is more profound for larger alcohols since less water-soluble larger alcohols are expelled more than shorter alcohols, and the gum is not a good adsorbent for alcohols.

The concentration of alcohols in the vapor phase starts to decrease as soon as binding sites become available for alcohols which is related to a decrease in water content. The results also indicate that completely dry gum powders would not adsorb alcohols except methanol. A possible explanation is that since the majority of binding sites is limited in size, larger alcohols are unable to interact with gum unless water causes swelling of the gum, thus exposing the binding sites. Small methanol molecules may be able to interact with gum without its swelling by water. Larger degree of swelling may be needed for larger alcohols to interact

with the gum as evidenced by the shifting of the minimum point of vapor concentration to a higher water content in the case of 1-butanol.

With a larger amount of 1-butanol in the system, the amount of the alcohol in the headspace increases at higher water content (low gum content). It is apparent that there are more free alcohol molecules which are easily vaporized as the alcohol/water ratio increases (Fig. 7). The point where the maximum increase occurs is shifted to a higher water content region with an increase in alcohol concentration due to a higher probability for the alcohol to interact with adsorption sites on the gum molecules.

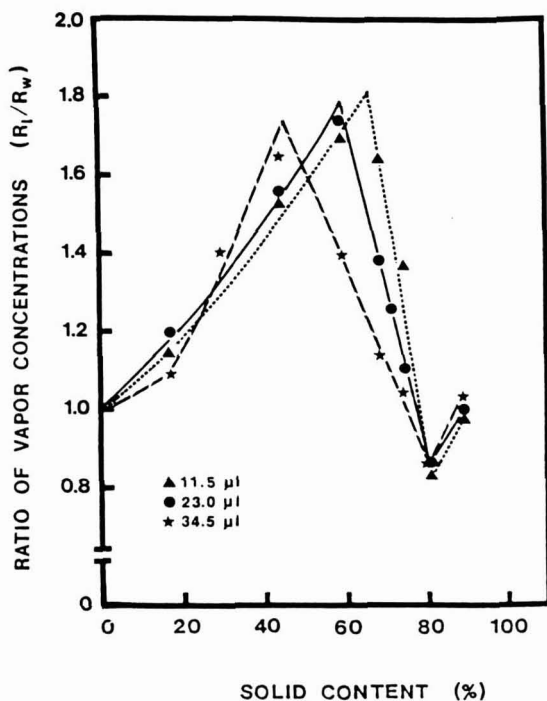


FIG. 7. EFFECTS OF N-BUTANOL CONCENTRATION ON VAPOR CONCENTRATION IN A SYSTEM CONTAINING VARIOUS LEVELS OF XANTHAN GUM

Shown in Fig. 8 are changes in headspace concentration of low molecular weight aliphatic alcohols caused by the presence of various amounts of maltodextrin which is commonly used as a bulking agent in food processing. Maltodextrins are expected to have similar effects on volatility of flavor compounds as xanthan gum, because both are mainly composed of hexose units. General shapes of the curves in Fig. 8 resemble those obtained for the gum, though, some differences have been found. First, there is less increase in alcohol

content in the vapor phase as molecular size increases from methanol to propanol. Secondly, 1-butanol is adsorbed to maltodextrin in almost the entire range of the solids content, and the changes in vapor concentration of 1-butanol are similar to those found with soy protein. Kieckbusch and King (1979) also found similar results with acetates in maltodextrin solutions. The authors reported that air-liquid partition coefficients of acetates increase with increasing maltodextrin concentration. However, as the molecular weight of acetate increases from methyl to butyl acetate, the extent of the increase in partition coefficient becomes smaller due to stronger affinity between acetates and maltodextrin, even though the presence of maltodextrin depresses the partition coefficient of pentyl acetate.

The larger the molecular size of alcohols, the weaker the interactions between alcohols and water. Thus, larger alcohols are expelled more from water to the vapor phase or to the solid phase, depending on the ability of the solids to adsorb alcohols. In the case of xanthan gum, alcohols are forced to the vapor phase because the gum adsorbs very little amounts of alcohols, resulting in an increase in their vapor concentration. The extent of the increase depends on the solubility of alcohols in water: i.e., the more soluble in water, the less alcohol in the vapor state. Maltodextrins apparently adsorb alcohols, possibly through physical entrapment or hydrophobic association. Maltodextrins in a solution may form aggregates of helical nature with the more hydrophobic portions existing inside. Thus, larger alcohols may be trapped inside of the helices or form hydrophobic association. Therefore, with maltodextrin in the system, the vapor concentration of alcohols is influenced not only by their solubility, but by interactions between alcohols and maltodextrin. These could cause a smaller increase in vapor concentration with larger alcohols or even a decrease with 1-butanol. The presence of ionic sites on xanthan gum molecules may prevent the formation of a tightly knitted network, thus inhibiting entrapment of alcohols.

With soy isolate in the system, there is little change in vapor concentration of methanol and ethanol until the soy content reaches 70%, after which point the concentration in the headspace decreases sharply (Fig. 9). However, 1-propanol and 1-butanol show an opposite trend. Their vapor concentrations continuously decrease as the soy content increases up to around 85%, and then increase with a further increase in the solids content. Since soy isolate has less sorption capacity for water than xanthan gum, a decrease in the amount of solvent water may not affect the vapor pressure of alcohols as profoundly as xanthan gum, resulting in very little changes for methanol and ethanol and a continuous drop in alcohol concentration for 1-propanol and 1-butanol in the vapor phase. Adsorption of alcohols increases with increasing the molecular size of alcohols. Less solubility and increased hydrophobicity may contribute towards the larger drop in vapor concentration of larger alcohols.

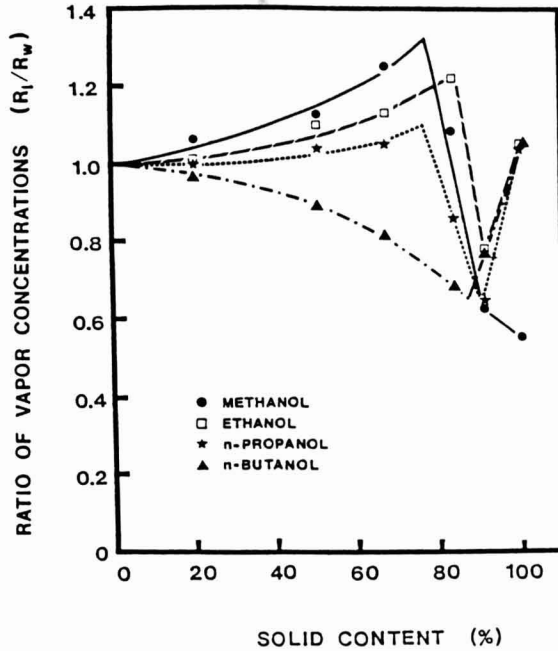


FIG. 8. CHANGES IN VAPOR CONCENTRATION OF ALCOHOLS AS A FUNCTION OF MALTODEXTRIN CONTENT

Franzen and Kinsella (1974) believed that the decrease in headspace concentration by proteins was due to the reduced surface area of the protein-flavor mixtures by the presence of water. However, the authors did not eliminate the possibility of effects by interactions between protein and flavor molecules. Data obtained in this study indicate that volatility of flavor compounds is affected by interactions of proteins not only with flavor compounds but also with water molecules.

At contents of soy protein above 80%, the magnitude of depression in vapor concentration by the protein becomes smaller for the two larger alcohols, whereas it increases continuously for the smaller alcohols. Therefore, it can be concluded that the presence of a certain amount of water may aid the binding of alcohols, especially for large alcohols, as they may require water to form hydrophobic interactions with proteins. Fukushima (1969) noted that hydrophobic regions of proteins in aqueous solutions could be easily disrupted by the addition of water soluble solvents which possess both hydrophobic and hydrophilic properties. The hydrophobic portions of the added solvents can penetrate into the hydrophobic regions only after disruption of the surrounding hydrophilic shell by water. The hydrophobicity of an alcohol is enhanced as

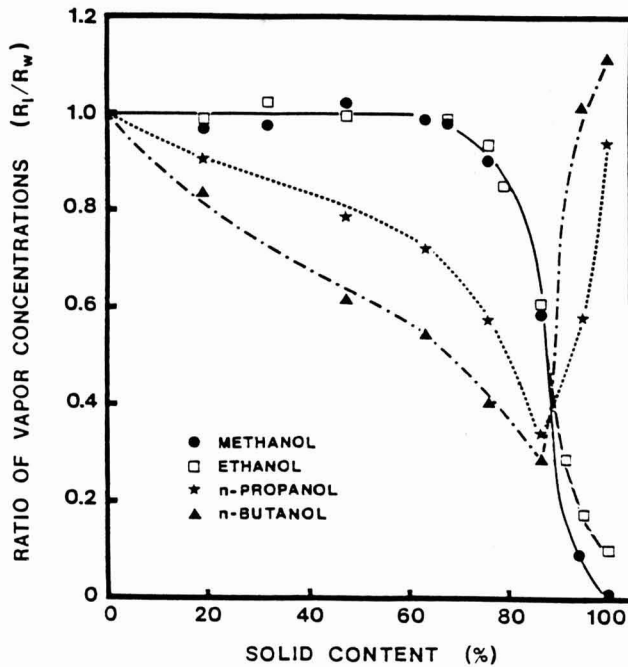


FIG. 9. CHANGES IN VAPOR CONCENTRATION OF ALCOHOLS AS A FUNCTION OF SOY PROTEIN ISOLATE CONTENT

chain length becomes longer, and thus longer chained alcohols interact easily with proteins. Methanol and ethanol may be small enough to penetrate into the interior of the protein structure to find further binding sites, even without disruption of the hydrophilic shell by water, resulting in a continuous decrease in their vapor concentration up to the dry state of the soy protein.

The extent of interactions between organic molecules and soy protein in a solution follows the denaturing power of a solvent system. More hydrophobic alcohols which are more effective denaturants interact more with protein. The interaction is affected by the water concentration. A small amount of water in a system increases interactions over a completely dry system, especially for larger alcohols. It is known that mixtures of water and alcohols have higher denaturing capacity than pure alcohols (Fukushima 1969). In summary, the interactions of alcohols with soy protein increase as the molecular size of the volatiles becomes larger. In a dry system of soy protein, on the other hand, adsorption of volatiles decreases with an increased molecular size since the binding sites on the protein are limited in size and shape.

Figures 10 and 11 show changes in vapor concentrations of ethanol and 1-butanol caused by a 1:1 mixture of soy protein and maltodextrin, along with

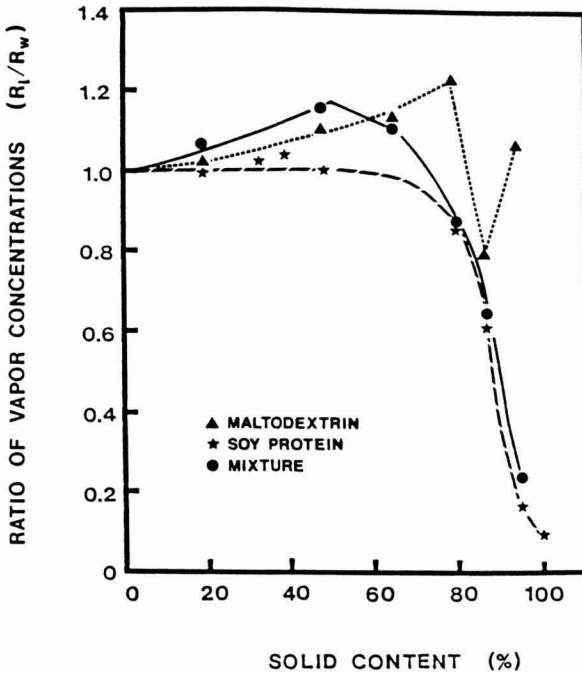


FIG. 10. CHANGES IN VAPOR CONCENTRATION OF ETHANOL AS INFLUENCED BY THE PRESENCE OF A MIXTURE OF MALTODEXTRIN AND SOY PROTEIN

the changes occurring when each powder is present separately. From both figures, it is obvious that the extent of changes by a mixture is not a simple average of those changes by each solid.

When both solids do not adsorb alcohol because water molecules already occupy binding sites (ethanol, up to 50% solids), the amount of alcohol in the headspace is higher than the amounts in either system, namely, soy protein or maltodextrin. If any solid is able to adsorb alcohol at a given condition, the percent decrease in vapor concentration of alcohol follows the values of the system containing this solid. It is, therefore, concluded that alcohols are preferentially adsorbed to the solid which has stronger affinity for the alcohol, and then any remaining alcohol molecules may interact with the second solid.

It has been found in this investigation that the composition of a food system greatly affects the volatility of flavor components. Various food solids interact with volatile compounds through different mechanisms, and the amount of water, being one of the major components in foods, also has a profound effect on the interactions. In the presence of a large amount of water, volatile molecules such as alcohols must compete with water for binding sites on food solids to form hydrogen bonding. Therefore, better water-adsorbing materials in solution

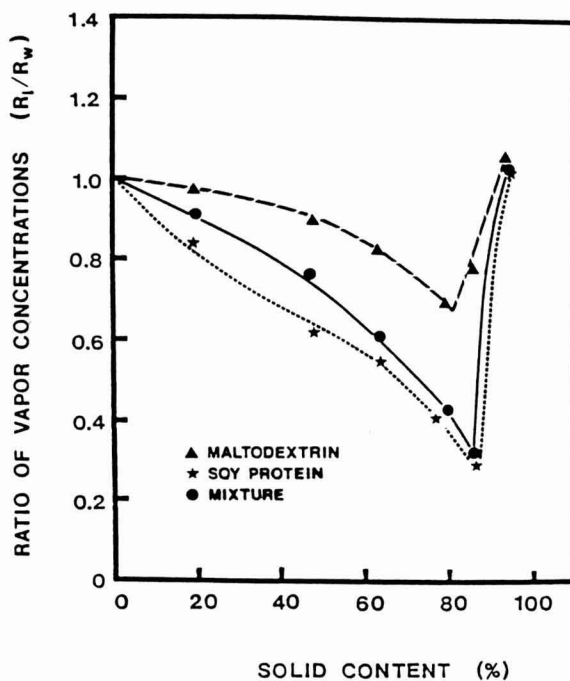


FIG. 11. CHANGES IN VAPOR CONCENTRATION OF N-BUTANOL AS INFLUENCED BY THE PRESENCE OF A MIXTURE OF MALTODEXTRIN AND SOY PROTEIN

such as xanthan gum exhibit little capacity for the binding of alcohols. However, longer chain alcohols, due to their increasing hydrophobicity, may adsorb onto hydrophobic sites on soy protein, maltodextrin and fumed silica. With this approach, it may become possible to predict, to some degree, the behavior of flavor compounds in relatively simple systems. The reported data may also be used to understand the mechanisms involved in volatile retention during various thermal processes.

ACKNOWLEDGMENTS

Funds to carry out this work were provided in part by the Cabot Corp., Tuscola Illinois, for which the authors are deeply indebted.

REFERENCES

- BUTLER, J.A.V., RAMCHANDANI, C.N. and THOMSON, D.W. 1935. The solubility of non-electrolytes. Part I. The free energy of hydration of some aliphatic alcohols. *J. Chem. Soc.* 280-285.
- BUTTERY, R.G., GUADAGNI, D.G. and OKANO, S. 1965. Air-water partition coefficients of some aldehydes. *J. Sci. Food Agric.* 16, 691-692.
- BUTTERY, R.G., LING, L.C. and GUADAGNI, D.G. 1969. Food volatiles. Volatilities of aldehydes, ketones, and esters in dilute water solution. *J. Agric. Food Chem.* 17, 385-389.
- BUTTERY, R.G., BOMBEN, J.L., GUADAGNI, D.G. and LING, L.C. 1971. Some considerations of the volatilities of organic flavor compounds in foods. *J. Agric. Food Chem.* 19, 1045-1048.
- CURTHOYS, G., DAVYDOV, V.Y., KISELEV, A.V., KISELEV, S.A. and KUZNETSOV, B.V. 1974. Hydrogen bonding in adsorption on silica. *J. Colloid Interface Sci.* 48, 58-72.
- FRANZEN, K.L. and KINSELLA, J.E. 1974. Parameters affecting the binding of volatile flavor compounds in model food systems. I. Proteins. *J. Agric. Food Chem.* 22, 675-678.
- FUKUSHIMA, D. 1969. Denaturation of soybean proteins by organic solvents. *Cereal Chem.* 46, 156-163.
- ILER, R.K. 1979. *Chemistry of Silica*, John Wiley & Sons, New York.
- JENNINGS, W.G. 1965. Influence of temperature and salt additions on vapor equilibration of headspace. *J. Food Sci.* 30, 445-449.
- KIECKBUSCH, T.G. and KING, C.J. 1979. Partition coefficients for acetates in food systems. *J. Agric. Food Sci.* 27, 504-507.
- KING, C.J. 1974. Novel dehydration techniques. In *Advance in Pre-concentration and Dehydration of Foods*, (A. Spicer, ed.) pp. 435-488. John Wiley & Sons, New York.
- KING, C.J. 1983. Physical and chemical properties governing volatilization of flavor and aroma components. In *Physical Properties of Foods*, (M. Peleg and E.B. Bagley, eds.) pp. 399-421. Van Nostrand Reinhold/AVI, New York.
- LEBERT, A. and RICHON, D. 1984. Infinite dilution activity coefficients of n-alcohols as a function of dextrin concentration in water-dextrin systems. *J. Agric. Food Chem.* 32, 1156-1161.
- MAIER, H.G. 1970. Volatile flavoring substances in foodstuffs. *Angew. Chem., Int. Ed.* 9, 917-926.
- MAZZA, G. 1980. Relative volatilities of some onion flavour components. *J. Food Technol.* 15, 35-41.
- NAWAR, W.W. 1971. Some variables affecting composition of headspace aroma. *J. Agric. Food Chem.* 19, 1057-1059.

- NELSON, P.E. and HOFF, J.E. 1968. Food volatiles: Gas chromatographic determination of partition coefficients in water-lipid systems. *J. Food Sci.* 33, 479-482.
- VITENBERG, A.G., IOFFE, B.V. and BORISOV, V.N. 1974. Application of phase equilibria to gas chromatographic trace analysis. *Chromatographia* 7, 610-619.
- VOILLEY, A., SIMATOS, D. and LONCIN, M. 1977. Gas phase concentration of volatiles in equilibrium with a liquid aqueous phase. *Lebensm.-Wiss. U.-Technol.* 10, 45-49.
- WEBER, JR., W.J. 1985. Adsorption theory, concepts, and models. In *Adsorption Technology*, (F.L. Slejko, ed.) pp. 1-35. Marcel Dekker, New York.
- WIENTJES, A.G. 1968. The influence of sugar concentration on the vapor pressure of food odor volatiles in aqueous solution. *J. Food Sci.* 33, 1-2.

**F
N
P**

PUBLICATIONS IN FOOD SCIENCE AND NUTRITION

Journals

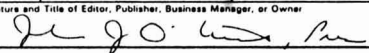
JOURNAL OF MUSCLE FOODS, N.G. Marriott and G.J. Flick, Jr.
JOURNAL OF SENSORY STUDIES, M.C. Gacula, Jr.
JOURNAL OF FOOD SERVICE SYSTEMS, O.P. Snyder, Jr.
JOURNAL OF FOOD BIOCHEMISTRY, J.R. Whitaker, N.F. Haard and
H. Swaisgood
JOURNAL OF FOOD PROCESS ENGINEERING, D.R. Heldman and R.P. Singh
JOURNAL OF FOOD PROCESSING AND PRESERVATION, D.B. Lund
JOURNAL OF FOOD QUALITY, R.L. Shewfelt
JOURNAL OF FOOD SAFETY, T.J. Montville and A.J. Miller
JOURNAL OF TEXTURE STUDIES, M.C. Bourne and P. Sherman

Books

NITRITE-CURED MEAT, R.G. Cassens
THE POTENTIAL FOR NUTRITIONAL MODULATION OF THE AGING
PROCESSES, D.K. Ingram *et al.*
CONTROLLED/MODIFIED ATMOSPHERE/VACUUM PACKAGING OF
FOODS, A.L. Brody
NUTRITIONAL STATUS ASSESSMENT OF THE INDIVIDUAL, G.E. Livingston
QUALITY ASSURANCE OF FOODS, J.E. Stauffer
THE SCIENCE OF MEAT AND MEAT PRODUCTS, 3RD ED., J.F. Price and
B.S. Schweigert
HANDBOOK OF FOOD COLORANT PATENTS, F.J. Francis
ROLE OF CHEMISTRY IN THE QUALITY OF PROCESSED FOODS,
O.R. Fennema, W.H. Chang and C.Y. Lii
NEW DIRECTIONS FOR PRODUCT TESTING AND SENSORY ANALYSIS
OF FOODS, H.R. Moskowitz
PRODUCT TESTING AND SENSORY EVALUATION OF FOODS,
H.R. Moskowitz
ENVIRONMENTAL ASPECTS OF CANCER: ROLE OF MACRO AND MICRO
COMPONENTS OF FOODS, E.L. Wynder *et al.*
FOOD PRODUCT DEVELOPMENT IN IMPLEMENTING DIETARY
GUIDELINES, G.E. Livingston, R.J. Moshy, and C.M. Chang
SHELF-LIFE DATING OF FOODS, T.P. Labuza
RECENT ADVANCES IN OBESITY RESEARCH, VOL. V, E. Berry,
S.H. Blondheim, H.E. Eliahou and E. Shafrir
RECENT ADVANCES IN OBESITY RESEARCH, VOL. IV, J. Hirsch *et al.*
RECENT ADVANCES IN OBESITY RESEARCH, VOL. III, P. Bjorntorp *et al.*
RECENT ADVANCES IN OBESITY RESEARCH, VOL. II, G.A. Bray
RECENT ADVANCES IN OBESITY RESEARCH, VOL. I, A.N. Howard
ANTINUTRIENTS AND NATURAL TOXICANTS IN FOOD, R.L. Ory
UTILIZATION OF PROTEIN RESOURCES, D.W. Stanley *et al.*
VITAMIN B₆: METABOLISM AND ROLE IN GROWTH, G.P. Tryfiates
HUMAN NUTRITION, 3RD ED., F.R. Mottram
FOOD POISONING AND FOOD HYGIENE, 4TH ED., B.C. Hobbs *et al.*
POSTHARVEST BIOLOGY AND BIOTECHNOLOGY, H.O. Hultin and M. Milner

Newsletters

FOOD INDUSTRY REPORT, G.C. Melson
FOOD, NUTRITION AND HEALTH, P.A. Lachance and M.C. Fisher
FOOD PACKAGING AND LABELING, S. Sacharow

U.S. Postal Service STATEMENT OF OWNERSHIP, MANAGEMENT AND CIRCULATION <small>Required by 39 U.S.C. 3685</small>			
1A. Title of Publication JOURNAL OF FOOD PROCESS ENGINEERING		1B. PUBLICATION NO. 0 1 4 5 8 8 7 6	2. Date of Filing Oct. 1, 1990
3. Frequency of Issue Quarterly		3A. No. of Issues Published Annually 4	3B. Annual Subscription Price \$98.00
4. Complete Mailing Address of Known Office of Publication (Street, City, County, State and ZIP+4 Code) (Not printers) 6527 Main St., POB 374, Trumbull, Fairfield, CT 06611			
5. Complete Mailing Address of the Headquarters of General Business Offices of the Publisher (Not printers) 6527 Main St., POB 374, Trumbull, CT 06611			
6. Full Name and Complete Mailing Address of Publisher, Editor, and Managing Editor (This item MUST NOT be blank)			
Publisher (Name and Complete Mailing Address) John J. O'Neil, 6527 Main St., POB 374, Trumbull, CT 06611			
Editor (Name and Complete Mailing Address) Dr. Dennis R. Heldman, National Food Processor's Association, 1401 New York Ave., NW, Washington, D.C. 20005			
Editor (Name and Complete Mailing Address) Dr. R. Paul Singh, Univ. of California, Dept. of Agricultural Eng., Davis, CA 95616			
7. Owners (If owned by a corporation, its name and address must be stated and also immediately thereunder the names and addresses of stockholders owning or holding 1 percent or more of total amount of stock. If not owned by a corporation, the names and addresses of the individual owners must be given. If owned by a partnership or other unincorporated firm, its name and address, as well as that of each individual must be given. If the publication is published by a nonprofit organization, its name and address must be stated.) (Item must be completed.)			
Full Name		Complete Mailing Address	
Food & Nutrition Press, Inc.		6527 Main St., POB 374, Trumbull, CT 06611	
John J. O'Neil		53 Stonehouse Rd., Trumbull, CT 06611	
Michael J. Tully		1 No. Slope Union Gap Village, Clinton, NJ 08809	
Kathryn O & Christopher R. Ziko		8 Maria Alicia Dr., Huntington, CT 06484	
John J. O'Neil, Jr.		115 Maureen St., Stratford, CT 06497	
8. Known Bondholders, Mortgagees, and Other Security Holders Owning or Holding 1 Percent or More of Total Amount of Bonds, Mortgages or Other Securities (If there are none, so state)			
Full Name		Complete Mailing Address	
None			
9. For Completion by Nonprofit Organizations Authorized to Mail at Special Rates (DMM Section 413.12 only) The purpose, function, and nonprofit status of the organization and the exempt status for Federal income tax purposes (Check one)			
<input type="checkbox"/> (1) Has Not Changed During Preceding 12 Months		<input type="checkbox"/> (2) Has Changed During Preceding 12 Months (If changed, publisher must submit explanation of change with this statement.)	
10. Extent and Nature of Circulation (See instructions on reverse side)		Average No. Copies Each Issue During Preceding 12 Months	Actual No. Copies of Single Issue Published Nearest to Filing Date
A. Total No. Copies (Net Press Run)		450	450
B. Paid and/or Requested Circulation			
1. Sales through dealers and carriers, street vendors and counter sales		0	0
2. Mail Subscription (Paid and/or requested)		267	299
C. Total Paid and/or Requested Circulation (Sum of 10B1 and 10B2)		267	299
D. Free Distribution by Mail, Carrier or Other Means (Samples, Complimentary, and Other Free Copies)		46	46
E. Total Distribution (Sum of C and D)		313	345
F. Copies Not Distributed			
1. Office use, left over, unaccounted, spoiled after printing		137	105
2. Return from News Agents		0	0
G. TOTAL (Sum of E, F1 and 2—should equal net press run shown in A)		450	450
11. I certify that the statements made by me above are correct and complete		Signature and Title of Editor, Publisher, Business Manager, or Owner 	

GUIDE FOR AUTHORS

Typewritten manuscripts in triplicate should be submitted to the editorial office. The typing should be double-spaced throughout with one-inch margins on all sides.

Page one should contain: the title, which should be concise and informative; the complete name(s) of the author(s); affiliation of the author(s); a running title of 40 characters or less; and the name and mail address to whom correspondence should be sent.

Page two should contain an abstract of not more than 150 words. This abstract should be intelligible by itself.

The main text should begin on page three and will ordinarily have the following arrangement:

Introduction: This should be brief and state the reason for the work in relation to the field. It should indicate what new contribution is made by the work described.

Materials and Methods: Enough information should be provided to allow other investigators to repeat the work. Avoid repeating the details of procedures which have already been published elsewhere.

Results: The results should be presented as concisely as possible. Do not use tables and figures for presentation of the same data.

Discussion: The discussion section should be used for the interpretation of results. The results should not be repeated.

In some cases it might be desirable to combine results and discussion sections.

References: References should be given in the text by the surname of the authors and the year. *Et al.* should be used in the text when there are more than two authors. All authors should be given in the Reference section. In the Reference section the references should be listed alphabetically. See below for style to be used.

DEWALD, B., DULANEY, J.T., and TOUSTER, O. 1974. Solubilization and polyacrylamide gel electrophoresis of membrane enzymes with detergents. In *Methods in Enzymology*, Vol. xxxii, (S. Fleischer and L. Packer, eds.) pp. 82-91, Academic Press, New York.

HASSON, E.P. and LATIES, G.G. 1976. Separation and characterization of potato lipid acylhydrolases. *Plant Physiol.* 57,142-147.

ZABORSKY, O. 1973. *Immobilized Enzymes*, pp. 28-46, CRC Press, Cleveland, Ohio.

Journal abbreviations should follow those used in *Chemical Abstracts*. Responsibility for the accuracy of citations rests entirely with the author(s). References to papers in press should indicate the name of the journal and should only be used for papers that have been accepted for publication. Submitted papers should be referred to by such terms as "unpublished observations" or "private communication." However, these last should be used only when absolutely necessary.

Tables should be numbered consecutively with Arabic numerals. The title of the table should appear as below:

Table 1. Activity of potato acyl-hydrolases on neutral lipids, galactolipids, and phospholipids
Description of experimental work or explanation of symbols should go below the table proper. Type tables neatly and correctly as tables are considered art and are not typeset. Single-space tables.

Figures should be listed in order in the text using Arabic numbers. Figure legends should be typed on a separate page. Figures and tables should be intelligible without reference to the text. Authors should indicate where the tables and figures should be placed in the text. Photographs must be supplied as glossy black and white prints. Line diagrams should be drawn with black waterproof ink on white paper or board. The lettering should be of such a size that it is easily legible after reduction. Each diagram and photograph should be clearly labeled on the reverse side with the name(s) of author(s), and title of paper. When not obvious, each photograph and diagram should be labeled on the back to show the top of the photograph or diagram.

Acknowledgments: Acknowledgments should be listed on a separate page.

Short notes will be published where the information is deemed sufficiently important to warrant rapid publication. The format for short papers may be similar to that for regular papers but more concisely written. Short notes may be of a less general nature and written principally for specialists in the particular area with which the manuscript is dealing. Manuscripts which do not meet the requirement of importance and necessity for rapid publication will, after notification of the author(s), be treated as regular papers. Regular papers may be very short.

Standard nomenclature as used in the engineering literature should be followed. Avoid laboratory jargon. If abbreviations or trade names are used, define the material or compound the first time that it is mentioned.

EDITORIAL OFFICES: DR. D.R. HELDMAN, COEDITOR, *Journal of Food Process Engineering*, National Food Processors Association, 1401 New York Avenue, N.W., Washington, D.C. 20005 USA; or DR. R.P. SINGH, COEDITOR, *Journal of Food Process Engineering*, University of California, Davis, Department of Agricultural Engineering, Davis, CA 95616 USA.

CONTENTS

Natural Convection Heat Transfer Between Non-Newtonian Fluids and an Irregular Shaped Particle A. ALHAMDAN and S.K. SASTRY	113
Oxygen Transmission Rate of an Edible Methylcellulose Palmitic Acid Film D.C. RICO-PENA and J.A. TORRES	125
An Approach to Study and Model the Hydrodynamic Cleaning Effect B.-O. BERGMAN and C. TRAGARDH	135
Mathematical Analysis of Critical Parameters in Aseptic Particulate Processing Systems J.W. LARKIN	155
Changes in Partition Coefficients of Alcohols as Affected by the Presence of Various Food Solids S. CHUNG and R. VILLOTA	169